Article

ESG Financial Market with Informed Traders within the Bachelier–Black–Scholes–Merton Model

Nancy Asare Nyarko [1,*], **Bhathiya Divelgama** [1], **Peter Yegon** [1],
W. Brent Lindquist [1], **Abootaleb Shirvani** [2], **Svetlozar T. Rachev** [1],
Frank J. Fabozzi [3]

[1] Department of Mathematics & Statistics, Texas Tech University, Lubbock, TX 79409, USA; bdivelga@ttu.edu (BD); pyegon@ttu.edu (PY); Brent.Lindquist@ttu.edu (WBL); Zari.Rachev@ttu.edu; (STR)

[2] Department of Mathematical Science, Kean University, Union, NJ 07083, USA; ashirvan@kean.edu (AS)

[3] Carey Business School, Johns Hopkins University, Baltimore, MD 21202, USA; fabozzi321@aol.com (FJF)

* Correspondence: Nancy Asare Nyarko, Email: nasareny@ttu.edu.

ABSTRACT

This study seeks to advance the theory of dynamic asset pricing by introducing asset valuation, adjusted by environmental, social and governance (ESG) ratings, within a unified Bachelier–Black–Scholes–Merton market model, and developing option valuation in both continuous-time and discrete-time (binomial pricing tree) frameworks. An empirical study based on call option prices for assets selected from the Nasdaq-100 develops implied values for the main ESG parameter in the pricing model. For these stocks, option traders have in-the-money ESG valuations that are lower than the spot price. Within the discrete-time framework, we demonstrate how an informed trader can adopt a futures trading strategy to optimize an effective dividend stream.

KEYWORDS: ESG finance; Bachelier's model; Black–Scholes–Merton model; option prices; binomial pricing trees

INTRODUCTION

Despite initial rejection of the Bachelier model [1], its arithmetic Brownian motion dynamics have found acceptance in certain areas. To combine the strengths of both arithmetic and geometric Brownian motion models, the classical Black–Scholes–Merton (BSM) model [2,3] has been merged with a modernized Bachelier (MB) model [4], producing a unified Bachelier–Black–Scholes–Merton (BBSM) model [5]. Both the unified model and its MB limit allow for price trajectories taking values in R, while, under the BSM limit, price processes take values in R^+. Exploiting the more extensive price range of the MB model, [4] developed a dynamic ESG-adjusted valuation ("ESG-adjusted pricing") for assets, which allows for stocks with low ESG ratings to be given a negative ESG-adjusted value.

A critical parameter of the adjusted valuation is the so-called ESG affinity, quantifying the market view of the "size" of the contribution of ESG ratings to asset values.

Consideration of ESG factors in financial modeling marks a paradigm shift in how asset values are assessed. As the world evolves toward a greener future, industry leaders must champion sustainability. (However, see [6] for a study of how sustainability efforts have varied by market). Providing a solid quantitative use for ESG ratings is an important step in the effort to champion sustainability in the financial world.

The use of ESG-adjusted prices alters the investment approach required for long-term investing, enabling ESG-conscious investors to more effectively measure, and (potentially) profit from, ESG strategies. Analyses based on such pricing must be woven into the investment processes of any discerning investor, as well as integrated into the corporate strategy of any company that is truly committed to increasing shareholder value [7].

This paper builds upon the following foundational papers. The work of [8] extended the BSM model to address option pricing in markets with informed traders, incorporating information about stock price direction and expected returns (As ESG-valued assets can take both positive and negative values, their BSM-based model for informed traders cannot be applied to ESG-valued markets). Using ESG-adjusted asset valuation as a motivation and example of the possibility of negative asset values, [4] developed the MB model, which corrects the defaults of previously published Bachelier models. Specifically the MB model defines a riskless asset that is theoretically consistent with the arithmetic Brownian motion dynamics of the risky asset and has a risk-free rate whose value can change between positive and negative over time. Additionally the risky asset price will not diverge to infinity if only a positive risk-free rate occurs. Asare Nyarko [9] explored fair valuation of ESG valued options under the MB model. The development of the unified BBSM model [5] thus presents the opportunity to extend ESG-valued markets with informed traders to a broader model which includes MB as one limiting case.

The first goal of this paper is to embed ESG asset valuation within the continuous-time BBSM model (Section 2: EMBEDDING ESG PRICING IN THE BBSM MODEL), placing ESG finance within the broader framework of a unified Bachelier and Black–Scholes–Merton theory. In Section 3 (BINOMIAL OPTION PRICING UNDER THE BBSM MODEL), we embed the ESG-adjusted asset valuation into the BBSM binomial option pricing model of [5].

The second goal is to provide an empirical study of discrete option pricing under the ESG-BBSM binomial model (Section 4: EMPIRICAL EXAMPLES: ESG-ADJUSTED PRICES AND PARAMETER FITTING). Our data set for 16 stocks selected from the Nasdaq-100 is described in Section 4.1 (The Data). Empirical examples of ESG-adjusted prices are presented in Section 4.2 (ESG-Adjusted Prices). In Section 4.3 (Parameter Fits) we describe how to fit the required parameters of the binomial model to empirical data. In Section 5 (THE IMPLIED ESG AFFINITY), using published call option prices for 01/02/2024, we compute implied values of the ESG affinity parameter as

functions of strike price and time to maturity. These can then be expressed in terms of an implied ESG valuation (as a function of strike price and time to maturity). Comparing the implied ESG valuation to financial spot prices provides insight into the views of option traders on the impact of ESG ratings on the underlying asset value.

The third goal of this study (Section 6: TRADING FORWARD CONTRACTS UTILIZING INFORMATION ON ASSET PRICE DIRECTION) focuses on a discrete-time, futures trading strategy that can be adopted by an option hedger (the trader taking a short position on an option) who may posses information regarding the future direction of movement of the ESG-adjusted valuation of the underlying stock. While the efficient market hypothesis argues that the direction of the asset price movement is unpredictable [10–18], numerous studies challenge this view and indicate that price direction may, indeed, be predictable [19–33]. As a result, [34–36] and many others have worked on understanding informed trading markets and the strategies employed. We demonstrate that the trader can optimize this trading strategy to produce an effective dividend stream.

Section 7 (CONCLUSION) concludes the paper with a discussion of future directions.

EMBEDDING ESG PRICING IN THE BBSM MODEL

Consider the market $(\mathcal{A}, \mathcal{B}, \mathcal{C})$ consisting of a risky asset $\mathcal{A}$, a riskless asset $\mathcal{B}$, and a European contingency claim (option) $\mathcal{C}$. Under BBSM, $\mathcal{A}$ has the price dynamics of a continuous-time diffusion process determined by the stochastic differential equation

$$dA_t = \varphi(A_t, t)dt + \psi(A_t, t)dB_t, \quad t \geq 0, \quad A_0 > 0,$$
$$\varphi(A_t, t) = a_t + \mu_t A_t, \qquad \psi(A_t, t) = v_t + \sigma_t A_t \tag{1}$$

where $B_t \in [0, \infty)$ is a standard Brownian motion on a stochastic basis

$$(\Omega, \mathcal{F}, F = \{\mathcal{F}_t = \sigma(B_u, u \leq t) \subseteq \mathcal{F}, t \geq 0\}, P) \tag{2}$$

of a complete probability space $(\Omega, \mathcal{F}, P)$. We assume that $(\Omega, \mathcal{F}_t, P)$ is a complete probability space for all $t \geq 0$ [37]. Note that P is a real-world probability measure.

In (1), $\varphi(A_t, t)$ is the price drift term and $\psi(A_t, t)$ is the price diffusion term. The coefficients satisfy $a_t \in R$, $\mu_t \in R$, $v_t \geq 0$, $\sigma_t \geq 0$, and are $\mathcal{F}$-adapted processes. The $\mathcal{F}$-adapted processes $\varphi(A_t, t)$ and $\psi(A_t, t)$ are assumed to satisfy the Lipschitz and growth conditions in $x \in R$ for $t \geq 0$ (see Section 5G and Appendix E of [38]). We also require $\int_0^t |\varphi(x, s)| \, ds < \infty$ and $\int_0^t |\psi(x, s)^2| \, ds < \infty$, $\forall t \geq 0$ and $x \in R$. To simplify the exposition, we will assume that a_t, μ_t, v_t, and σ_t have trajectories that are continuous and uniformly bounded on $t \in [0, \infty)$ P-almost surely (P-a.s.).

Lindquist [5] define the appropriate price dynamics of the riskless asset $\mathcal{B}$ (any other choice will result in a riskless asset whose dynamics are inconsistent with that of the risky asset) in the BBSM market model as

$$d\beta_t = \chi(\beta_t, t)dt, \quad \chi(\beta_t, t) = \rho_t + r_t\beta_t, \quad t \geq 0, \quad \beta_0 > 0 \tag{3}$$

Again, $\rho_t \in R$ and $r_t \in R$ are $\mathcal{F}$-adapted processes. The $\mathcal{F}$-adapted process $\chi(\beta_t, t)$ is also assumed to satisfy the Lipschitz and growth conditions in x, as well as the condition of absolute integrability. To simplify the exposition, we will assume that ρ_t and r_t have trajectories that are continuous and uniformly bounded on $t \in [0, \infty)$ P-a.s. The MB model is achieved as the limiting case $\mu_t = \sigma_t = r_t = 0$, while the classical BSM model is the limiting case $a_t = v_t = \rho_t = 0$. For brevity, we adopt the notation $\varphi_t = \varphi(A_t, t)$, $\psi_t = \psi(A_t, t)$ and $\chi_t = \chi(\beta_t, t)$. We require $\psi_t > 0$, P-a.s. A necessary condition for no-arbitrage is the requirement that $\beta_t \le A_t$, P-a.s.

Under the no-arbitrage assumption, the market price of risk is

$$\Theta_t = \frac{\varphi_t - \chi_t}{\psi_t} \tag{4}$$

which is strictly positive P-a.s. for all $t \ge 0$ providing $\varphi_t > \chi_t$, P-a.s.

The option $\mathcal{C}$ has the price dynamics

$$C_t = f(A_t, t), \quad t \in [0, T] \tag{5}$$

where $f(x, t)$, $x \in R$, $t \in [0, T]$, has continuous partial derivatives $\partial^2 f(x, t)/\partial x^2$ and $\partial f(x, t)/\partial t$ on $t \in [0, T)$, and T is the expiration (maturity) time of $\mathcal{C}$. The option's maturity payoff is $C_T = g(A_T)$ for some continuous function $g : R \to R$. The risk-neutral valuation of C_t is [5]

$$C_t = E_t^Q \left[\exp \left(-\int_t^T \left(r_u + \frac{\rho_u}{\beta_u} \right) du \right) g(A_T) \right], \quad t \in [0, T] \tag{6}$$

where $Q \sim P$ is the equivalent martingale measure and the asset price dynamics under Q is

$$dA_t = \left(r_t + \frac{\rho_t}{\beta_t} \right) A_t dt + \psi_t dB_t^Q, \quad t \ge 0 \tag{7}$$

In equation (6), B_t^Q, $t \in [0, \infty)$, is a standard Brownian motion on the stochastic basis $(\Omega, \mathcal{F}, F, Q)$.

Consider a published ESG rating (score) $Z_t^{(X)} \in [0, 10]$ for a company X at time t. Typically the scores $Z_t^{(X)}$ are on a zero-to-ten or a zero-to-one-hundred scale. Our data provider, Bloomberg Professional Services, uses the zero-to-ten scale. Rachev [4] argue that bounded scales for an ESG score do not differentiate adequately between the amount of effort that a company must undergo to raise their score above a current value. The amount of effort to raise an ESG score from 0 to 0.5 is trivial compared to the effort required to raise a score from 9.5 to 10.0. They further argue that scores based upon a convex, monotonically increasing function better represent such effort, and that the choice of such a function should be based ultimately on an axiomatic approach. In the absence of such an approach, they proposed the relative ESG measure

$$Z_t^{(X;I)} = \frac{Z_t^{(X)} - Z_t^{(I)}}{Z_t^{(I)}} \tag{8}$$

where $Z_t^{(X)}$ is the ESG rating (score) of company X and $Z_t^{(I)}$ is the ESG score of a relevant market index I. The value of $Z_t^{(X;I)}$ is independent of the range of the scale as long as the range is finite and the same range is used for both $Z_t^{(X)}$ and $Z_t^{(I)}$. They further define the ESG-adjusted stock price of company X at time $t \geq 0$ by

$$A_t = S_t^{(X)}(1 + \gamma^{\text{ESG}} Z_t^{(X;I)}) \tag{9}$$

which incorporates ESG scores as part of an asset's valuation. Here $S_t^{(X)} > 0$ represents the financial price of an asset, while $A_t \in R$ represents an ESG-adjusted valuation, which [4] refer to as the ESG-adjusted price. In our view, this relative ESG score (which, like return and risk-measure, is dimensionless) adds a third dimension to conventional risk - return analysis of dynamic asset prices. In equation (9), $\gamma^{\text{ESG}} \in R$ is referred to as the ESG affinity of the financial market. The ESG affinity is expected to change slowly with time (see Endnote 1 of [4]). Here we assume it is constant over the both the historical window of prices and the option price maturity times considered.

The ESG-adjusted stock price (equation (9)) can be negative. This is not surprising as the relative score $Z_t^{(X;I)}$ is analogous to any financial 'spread'. Hence [4] argued that the MB model, rather than BSM, is better designed to capture the trajectories of ESG-adjusted prices. We note the following dependencies of A_t on γ^{ESG}.

$$A_t = S_t^{(X)} + \gamma^{\text{ESG}} \left(S_t^{(X)} Z_t^{(X;I)} \right) \tag{10a}$$

$$A_{t+1} - A_t = S_{t+1}^{(X)} - S_t^{(X)} + \gamma^{\text{ESG}} \left(S_{t+1}^{(X)} Z_{t+1}^{(X;I)} - S_t^{(X)} Z_t^{(X;I)} \right) \tag{10b}$$

$$E[A_t] = E\left[S_t^{(X)} \right] + \gamma^{\text{ESG}} E\left[S_t^{(X)} Z_t^{(X;I)} \right] \tag{10c}$$

$$\text{Var}[A_t] = \text{Var}\left[S_t^{(X)} \right] + 2\gamma^{\text{ESG}} \text{Cov}\left[S_t^{(X)}, S_t^{(X)} Z_t^{(X;I)} \right] + (\gamma^{\text{ESG}})^2 \text{Var}\left[S_t^{(X)} Z_t^{(X;I)} \right] \tag{10d}$$

From (10a) through (10d), we see that changing the value of γ^{ESG} only affects the (additional) fractional financial price term $Z_t^{(X;I)} S_t^{(X)}$, which satisfies $|Z_t^{(X;I)} S_t^{(X)}| \leq S_t^{(X)}$.

BINOMIAL OPTION PRICING UNDER THE BBSM MODEL

Lindquist ([5] , Section 7) developed a binomial option pricing model under the BBSM model. We briefly summarize that model here. Consider a BBSM market $(\mathcal{A}, \mathcal{B}, \mathcal{C})$ consisting of the risky asset (stock) $\mathcal{A}$, the $\mathcal{B}$ and call option $\mathcal{C}$. The stock price A_t evolves according to the binomial pricing tree

$$A_{(k+1)\Delta,n} = \begin{cases} A_{(k+1)\Delta,n}^{(u)} = A_{k\Delta,n} + u_{k\Delta,n}, & \text{if } \zeta_{k+1,n} = 1, \\ A_{(k+1)\Delta,n}^{(d)} = A_{k\Delta,n} + d_{k\Delta,n}, & \text{if } \zeta_{k+1,n} = 0 \end{cases} \tag{11}$$

In equation (11), $A_{k\Delta,n}$, $k = 0, 1, \ldots, n$, $n \in N = \{1, 2, \ldots\}$, is the stock price at time $k\Delta$, $\Delta = \Delta_n = T/n$ where T is the fixed maturity time and $A_0 > 0$. For every $n \in N$, $\zeta_{k,n}$, $k = 1, 2, \ldots, n$, are independent, identically distributed

Bernoulli random variables with $P(\zeta_{k,n} = 1) = 1 - P(\zeta_{k,n} = 0) = p_n$ determining the filtration

$$F^{(n)} = \left\{ \mathcal{F}_k^{(n)} = \sigma(\zeta_{j,n} : j = 1, \ldots, k), \ \mathcal{F}_0^{(n)} = \{\emptyset, \Omega\}, \ \zeta_{0,n} = 0 \right\} \tag{12}$$

of the stochastic basis $(\Omega, \mathcal{F}, F^{(n)}, P)$ on the complete probability space $(\Omega, \mathcal{F}, P)$.

The riskless asset $\mathcal{B}$ has the discrete price dynamics

$$\beta_{(k+1)\Delta,n} = \beta_{k\Delta,n} + \chi_{k\Delta,n}\Delta, \quad k = 0, 1, \ldots, n-1, \quad \beta_{0,n} > 0 \tag{13}$$

where $\chi_{k\Delta,n}$ is the instantaneous rate of equation (3) at times $k\Delta$.

Under BBSM, price changes, rather than returns, are of primary interest. Let

$$c_{(k+1)\Delta,n} = A_{(k+1)\Delta,n} - A_{k\Delta,n}, \quad k = 0, \ldots, n-1, \quad c_{0,n} = 0 \tag{14}$$

Then,

$$c_{(k+1)\Delta,n} = \begin{cases} c_{(k+1)\Delta,n}^{(u)} = u_{k\Delta,n}, & \text{with probability (w.p.)} \quad p_n, \\ c_{(k+1)\Delta,n}^{(d)} = d_{k\Delta,n}, & \text{w.p.} \quad 1 - p_n \end{cases} \tag{15}$$

In order that the càdlàg process on the Skorokhod space $D[0, T]$ generated by the binomial tree (equation (11)) converge weakly to the continuous time process (equation (1)), we require that the conditional mean and variance satisfy

$$E[c_{(k+1)\Delta,n} \mid \mathcal{F}_k^{(n)}] = \varphi_{k\Delta,n}\Delta, \quad \text{Var}[c_{(k+1)\Delta,n} \mid \mathcal{F}_k^{(n)}] = \psi_{k\Delta,n}^2 \Delta \tag{16}$$

where $\varphi_{k\Delta,n}$ and $\psi_{k\Delta,n}^2$ are the instantaneous mean and variance of equation (7) at time $k\Delta$. Then $u_{k\Delta,n}$ and $d_{k\Delta,n}$ are given by

$$u_{k\Delta,n} = \varphi_{k\Delta,n}\Delta + \sqrt{\frac{1-p_n}{p_n}}\psi_{k\Delta,n}\sqrt{\Delta}, \qquad d_{k\Delta,n} = \varphi_{k\Delta,n}\Delta - \sqrt{\frac{p_n}{1-p_n}}\psi_{k\Delta,n}\sqrt{\Delta} \tag{17}$$

The option $\mathcal{C}$ has the discrete price dynamics $C_{k\Delta,n} = C(A_{k\Delta,n}, k\Delta)$, $k = 0, \ldots, n-1$. Consider a self-financing strategy, $P_{k\Delta,n} = a_{k\Delta,n}A_{k\Delta,n} + b_{k\Delta,n}\beta_{k\Delta,n}$ replicating the option price process $C_{k\Delta,n}$. The standard no-arbitrage arguments lead to the system

$$a_{k\Delta,n}A_{k\Delta,n} + b_{k\Delta,n}\beta_{k\Delta,n} = C_{k\Delta,n} \tag{18a}$$

$$a_{k\Delta,n}A_{(k+1)\Delta,n}^{(u)} + b_{k\Delta,n}\beta_{(k+1)\Delta,n} = C_{(k+1)\Delta,n}^{(u)} \tag{18b}$$

$$a_{k\Delta,n}A_{(k+1)\Delta,n}^{(d)} + b_{k\Delta,n}\beta_{(k+1)\Delta,n} = C_{(k+1)\Delta,n}^{(d)} \tag{18c}$$

Solution of equations (18b) and (18c) yields

$$a_{k\Delta,n} = \frac{C_{(k+1)\Delta,n}^{(u)} - C_{(k+1)\Delta,n}^{(d)}}{u_{k\Delta,n} - d_{k\Delta,n}},$$

$$b_{k\Delta,n} = \frac{1}{\beta_{k\Delta,n} + \chi_{k\Delta,n}\Delta}\left(C_{(k+1)\Delta,n}^{(u)} - \frac{C_{(k+1)\Delta,n}^{(u)} - C_{(k+1)\Delta,n}^{(d)}}{u_{k\Delta,n} - d_{k\Delta,n}}A_{(k+1)\Delta,n}^{(u)} \right) \tag{19}$$

Finally, solution of equation (18a) provides the risk-neutral valuation of the option given by the recursion

$$C_{k\Delta,n} = \frac{\beta_{k\Delta,n}}{\beta_{k\Delta,n} + \chi_{k\Delta,n}\Delta} \left(q_{k\Delta,n} C^{(u)}_{(k+1)\Delta,n} + (1 - q_{k\Delta,n}) C^{(d)}_{(k+1)\Delta,n} \right) \tag{20}$$

where the risk-neutral probability $q_{k\Delta,n}$ is

$$q_{k\Delta,n} = p_n - \frac{\varphi_{k\Delta,n} - \frac{\chi_{k\Delta,n}}{\beta_{k\Delta,n}} A_{k\Delta,n}}{\psi_{k\Delta,n}} \sqrt{p_n(1 - p_n)\Delta} \tag{21}$$

The limit $a_{k\Delta,n} = v_{k\Delta,n} = \rho_{k\Delta,n} = 0$ of equation (20) and equation (21) produces the option price recursion relation for the BSM model,

$$C_{k\Delta,n} = \frac{1}{1 + r_{k\Delta,n}\Delta} \left(q_{k\Delta,n} C^{(u)}_{(k+1)\Delta,n} + (1 - q_{k\Delta,n}) C^{(d)}_{(k+1)\Delta,n} \right) \tag{22}$$

having risk-neutral probability

$$q_{k\Delta,n} = p_n - \theta_{k\Delta,n} \sqrt{p_n(1 - p_n)\Delta} \tag{23}$$

where $\theta_{k\Delta,n}$ is the discrete form of the market price of risk, $\theta_t = (\mu_t - r_t)/\sigma_t$, $t \geq 0$, in the BSM model (in agreement with [8]). In this limit, the discrete price of the riskless asset obeys, $\beta_{k\Delta,n} = \beta_0 \prod_{j=0}^{k-1}(1 + r_{j\Delta,n}\Delta)$.

The limit $\mu_{k\Delta,n} = \sigma_{k\Delta,n} = r_{k\Delta,n} = 0$, produces the option price recursion relation for the [4] Bachelier model,

$$C_{k\Delta,n} = \frac{\beta_{k\Delta,n}}{\rho_{k\Delta,n} + \beta_{k\Delta,n}} \left(q_{k\Delta,n} C^{(u)}_{(k+1)\Delta,n} + (1 - q_{k\Delta,n}) C^{(d)}_{(k+1)\Delta,n} \right) \tag{24}$$

The risk-neutral probability $q_{k\Delta,n}$ is (see also [8]),

$$q_{k\Delta,n} = p_n - \frac{a_{k\Delta,n} - \frac{\rho_{k\Delta,n}}{\beta_{k\Delta,n}} A_{k\Delta,n}}{v_{k\Delta,n}} \sqrt{p_n(1 - p_n)\Delta} \tag{25}$$

In this limit, the discrete price of the riskless asset obeys $\beta_{k\Delta,n} = \beta_0 + \sum_{j=0}^{k-1} \rho_{j\Delta,n}\Delta$.

The Binomial Model is Not Recombining

A careful analysis shows that the risky-asset asset price process (equation (11)) does not, in fact, form a recombining tree. For a fixed value of k, $k = 0, 1, ..., n$, the superscripts (u) and (d) determine node "level" values at time $k + 1$. For a recombining binomial tree, at time k, there are $k + 1$ level numbers. Thus each node on the tree is indexed by a k, j pair, $k = 0, ..., n$, $j = 1, ..., k + 1$. With the inclusion of level numbers, equation (11) is written as

$$\begin{aligned} A^{j+1}_{(k+1)\Delta,n} &= A^j_{k\Delta,n} + u^j_{k\Delta,n}, &\text{w.p. } p, \\ A^j_{(k+1)\Delta,n} &= A^j_{k\Delta,n} + d^j_{k\Delta,n}, &\text{w.p. } 1 - p \end{aligned} \tag{26}$$

where, from equation (17),

$$u^j_{k\Delta,n} = \varphi^j_{k\Delta,n}\Delta + p^{(u)}\psi^j_{k\Delta,n}\sqrt{\Delta}, \qquad d^j_{k\Delta,n} = \varphi^j_{k\Delta,n}\Delta - p^{(d)}\psi^j_{k\Delta,n}\sqrt{\Delta},$$

$$\varphi^j_{k\Delta,n} = a + \mu A^j_{k\Delta,n}, \qquad \psi_{k\Delta,n} = v + \sigma A^j_{k\Delta,n},$$

$$p^{(u)} = \sqrt{\frac{1-p_n}{p_n}}, \qquad p^{(d)} = \sqrt{\frac{p_n}{1-p_n}} \tag{27}$$

Figure 1 illustrates a price configuration on four nodes of the tree, with time and level values indicated. Substituting equation (27) into equation (26) gives

$$A^{j+1}_{(k+1)\Delta,n} = \alpha^+ A^j_{k\Delta,n} + \eta^+, \qquad \text{w.p. } p,$$

$$A^j_{(k+1)\Delta,n} = \alpha^- A^j_{k\Delta,n} + \eta^-, \qquad \text{w.p. } 1-p \tag{28}$$

where

$$\alpha^+ = 1 + \mu\Delta + p^{(u)}\sigma\sqrt{\Delta}, \qquad \eta^+ = a\Delta + p^{(u)}v\sqrt{\Delta},$$

$$\alpha^- = 1 + \mu\Delta - p^{(d)}\sigma\sqrt{\Delta}, \qquad \eta^- = a\Delta - p^{(d)}v\sqrt{\Delta} \tag{29}$$

Note that α^+, α^-, η^+, and η^- are constants.
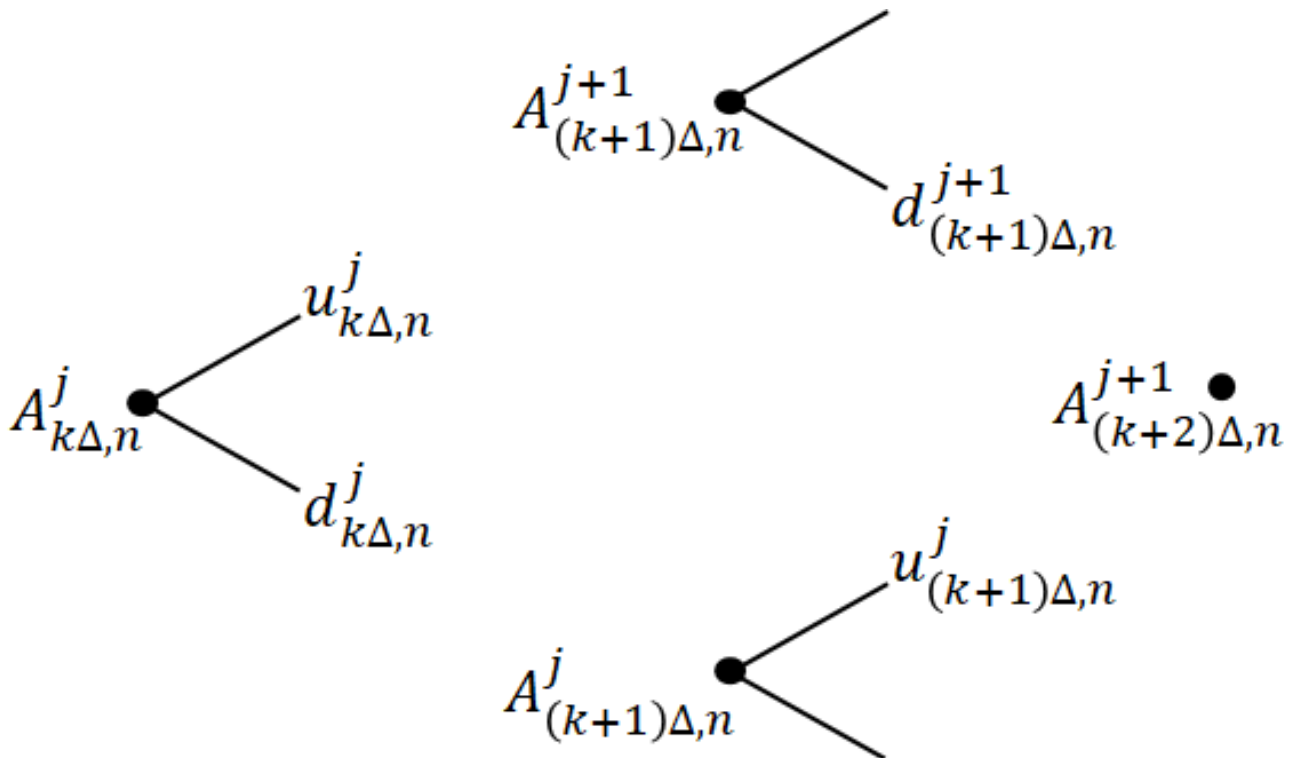
Figure 1. Time and level notation for the price evolution of the risky asset on the BBSM binomial tree.

For the tree to be recombining, in Figure 1 we must have

$$A_{(k+2)\Delta,n}^{j+1} = \alpha^+ A_{(k+1)\Delta,n}^{j} + \eta^+ = \alpha^- A_{(k+1)\Delta,n}^{j+1} + \eta^- \tag{30}$$

With some algebra, the difference

$$\epsilon = \left(\alpha^+ A_{(k+1)\Delta,n}^{j} + \eta^+ \right) - \left(\alpha^- A_{(k+1)\Delta,n}^{j+1} + \eta^- \right) \tag{31}$$

can be shown to be

$$\epsilon = \frac{a\sigma - v\mu}{\sqrt{p_n(1-p_n)}} \Delta^{3/2} \tag{32}$$

independent of time or level number. None-the-less, these constant errors propagate multiplicatively along the tree. To ensure that the tree is numerically recombining in our empirical work in Section 4, we define

$$A_{(k+2)\Delta,n}^{j+1} = 0.5 \left(\alpha^+ A_{(k+1)\Delta,n}^{j} + \eta^+ + \alpha^- A_{(k+1)\Delta,n}^{j+1} + \eta^- \right) \tag{33}$$

We note that ϵ vanishes more rapidly than $\sqrt{\Delta}$ and Δ terms as $\Delta \downarrow 0$. However, theoretical work remains to be done to ascertain whether the càdlàg process on the Skorokhod space $D[0,T]$ generated by either equation (11) or equation (33) does indeed converge weakly to the continuous time process (equation (1)). We leave this question open for further investigation. We do note that the BSM and MB limits of the price process (equation (11)) are indeed recombining (binomial) trees whose generated càdlàg processes do converge weakly to the appropriate BSM and MB limits of the continuous time process (equation (1)).

EMPIRICAL EXAMPLES: ESG-ADJUSTED PRICES AND PARAMETER FITTING

The Data

Table 1 provides brief summaries of the 16 companies in the Nasdaq-100 index (^NDX) as of 01/02/2024 that we considered for our empirical study. The stocks were chosen to represent the full range of ESG scores. Adjusted closing prices for the period 01/04/2016 through 01/02/2024 were obtained for these stocks [39] (accessed 01/02/2024). ESG scores for all 101 asset class shares in ^NDX were obtained from Bloomberg Professional Services (accessed 01/02/2024). Bloomberg provides "fiscal year (FY)" ESG scores. On 01/02/2024, yearly ESG scores were available for FY 2015 through FY 2022; scores for FY 2023 had not yet been released. Therefore the ESG scores for FY 2023 were set equal to those for FY 2022. Individual stock weights for the exchange traded fund (ETF) Invesco QQQ Trust (QQQ), were used as proxies for actual ^NDX weights [40] (accessed 01/02/2024). In our view this is a preferable choice for the weights as the ETF is a tradable instrument that is designed to track the ^NDX.

Table 1. Summaries of the 16 stocks used in the empirical study.

Ticker	Company Name	GICS Sector	Headquarters
AAPL	Apple Inc.	I.T.	Cupertino, CA
AMAT	Applied Materials, Inc.	I.T.	Santa Clara, CA
AMD	Advanced Micro Devices, Inc.	I.T.	Santa Clara, CA
AMZN	Amazon.com, Inc.	C.D.	Bellevue, WA
ASML	ASML Holding NV	I.T.	Veldhoven, NL
CSX	CSX Corp.	I	Jacksonville, FL
DLTR	Dollar Tree, Inc.	C.D.	Chesapeake, VA
EA	Electronic Arts, Inc.	C.S.	Redwood City, CA
GOOGL	Alphabet, Inc.	C.S.	Mountain View, CA
INTC	Intel Corp.	I.T.	Santa Clara, CA
NVDA	Nvidia Corp.	I.T.	Santa Clara, CA
PANW	Palo Alto Networks, Inc.	I.T.	Santa Clara, CA
ROST	Ross Stores, Inc.	C.D.	Dublin, CA
TEAM	Atlassian Corp.	I.T.	Sydney, AU
WDAY	Workday, Inc.	I.T.	Pleasanton, CA
WBD	Warner Bros Discovery, Inc.	C.S.	New York, NY

Note: GICS sector abbreviations: I.T. = Information Technology, C.D. = Consumer Discretionary, I = Industrials, C.S. = Communication Services.

Using the QQQ weights, a weighted ESG score for ^NDX was computed for each fiscal year. Figure 2 shows the resultant fiscal year, relative ESG scores $Z_t^{(X;\text{^NDX})}$ of the 16 chosen companies. Seven of the stocks have positive relative ESG scores over the entire 8 years of data; eight have negative relative ESG scores; and only one, PANW, has an ESG score that increases from below the index value to above. We note that, with the exception of PANW, the change in the ESG score of most companies relative to the index weighted average has remained approximately constant, or decreased, since 2019.

The ESG data were smoothed to provide daily values. Specifically we smoothed the values of $Z_t^{(X;\text{^NDX})}$. The fiscal year values were assigned to the last day (December 31) of the year (with the ESG score for 01/02/2024 being set equal to the 12/31/2022 value). The daily smoothing, which consisted of two steps: linear interpolation followed by a Gaussian-weighted, moving average smoothing function, provided daily values between 12/31/2015 and 01/02/2024. The linear interpolation produced daily values between successive year end values. The Gaussian-weighted, moving average produced a smoother $Z_t^{(X;\text{^NDX})}$ curve having the property that it produces no data "overshoot" or "undershoot". Figure 3 shows an example of the smoothing for $Z_t^{(\text{AAPL};\text{^NDX})}$.
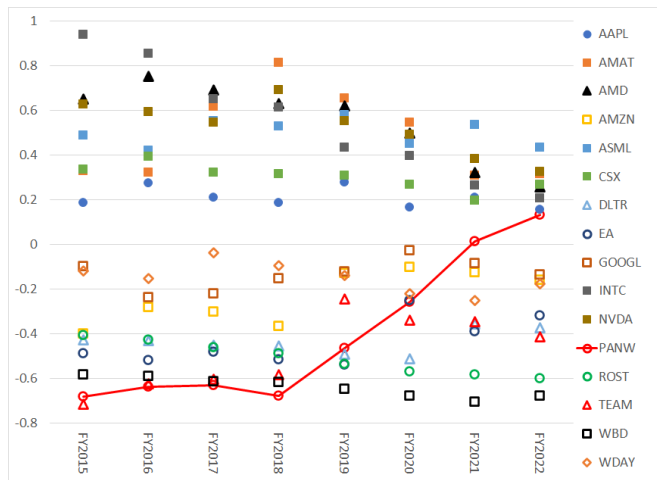
Figure 2. The relative ESG scores $Z_t^{(X;\text{^NDX})}$ of the 16 chosen companies.
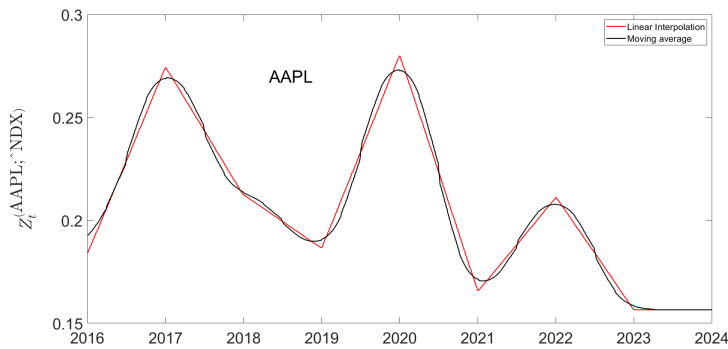
Figure 3. Illustration of the two-step smoothing process for $Z_t^{(\text{AAPL};\text{^NDX})}$.

ESG-Adjusted Prices

In Section 5, implied values for γ^{ESG} were estimated from call option prices, reflecting the view of option traders. However, there is no estimate for values of γ^{ESG} based upon historical spot trading. In order to investigate historical ESG-adjusted prices, we proceeded as follows. We assumed that the financial price series $S_t^{(X)}$ for each stock X over the historical time period 01/04/2016 though 01/02/2024 is a semi-martingale – most probably a Lévy process. Using the historical price series, we computed the time series of ESG-adjusted prices $A_t(\gamma^{\text{ESG}})$ (equation (9)) over the range of parameter values $\gamma^{\text{ESG}} \in [-5, 5]$. This bounding range correlates strongly with our requirement that the signal-to-noise ratio s:n(γ^{ESG}) lie within 5% of the value s:n(0); see Table A1.

For each value of γ^{ESG}, we determined the signal:noise ratio, s:n(γ^{ESG}), of $A_t(\gamma^{\text{ESG}})$. Figure 4 shows plots of s:n(γ^{ESG}) for four example stocks, illustrating a range of behaviors.

Defining γ_l^{ESG} and γ_u^{ESG} by

$$\gamma_l^{\text{ESG}} = \max \left\{ \gamma^{\text{ESG}} < 0 \; : \; \left| \frac{\text{s:n}(\gamma^{\text{ESG}})}{\text{s:n}(0)} - 1 \right| = 0.05, \right\},$$

$$\gamma_u^{\text{ESG}} = \min \left\{ \gamma^{\text{ESG}} > 0 \; : \; \left| \frac{\text{s:n}(\gamma^{\text{ESG}})}{\text{s:n}(0)} - 1 \right| = 0.05, \right\}$$

(34)

determines a range $\gamma^{\text{ESG}} \in [\gamma_l^{\text{ESG}}, \gamma_u^{\text{ESG}}]$ of values for which s:n(γ^{ESG}) lies within 5% of the value s:n(0). If the s:n ratio of the ESG-adjusted price $A_t(\gamma^{\text{ESG}})$ are larger than this range, there is the possibility that the time series will no longer be a semimartingale. This does not imply an assumption that $A_t(\gamma^{\text{ESG}})$ is not a semimartingale if γ^{ESG} falls outside of the range $[\gamma_l^{\text{ESG}}, \gamma_u^{\text{ESG}}]$.
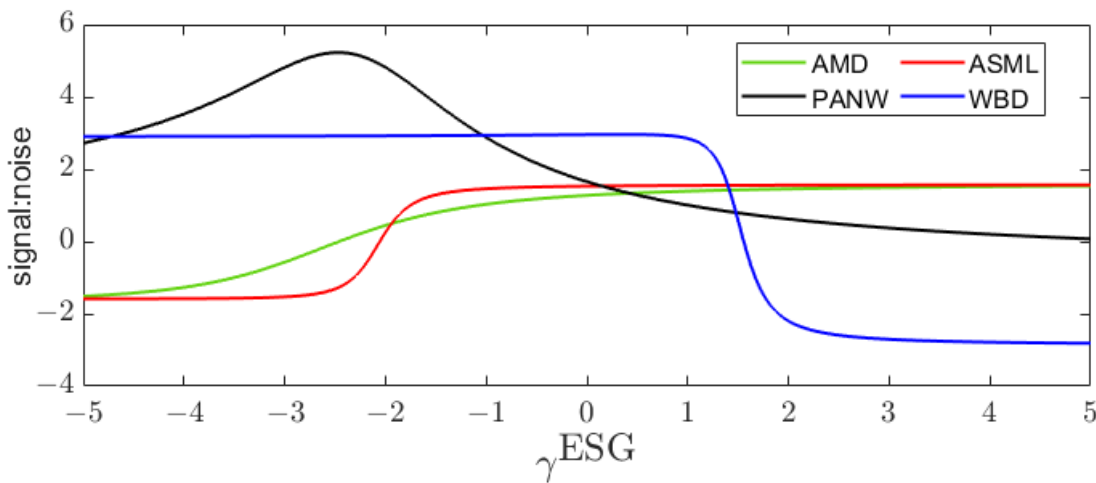
Figure 4. Signal:noise ratio as a function of γ^{ESG}.

The range $[\gamma_l^{\text{ESG}}, \gamma_u^{\text{ESG}}]$ found for each stock is given in Table A1 in Appendix A . The ranges vary, sometimes significantly. For the four stocks represented in Figure 4, Figure 5 plots the ESG-adjusted price series for $\gamma^{\text{ESG}} \in \{\gamma_l^{\text{ESG}}, 0, \gamma_h^{\text{ESG}}\}$. For PANW, the s:n ratio changes rapidly near $\gamma^{\text{ESG}} = 0$, and the range $[\gamma_l^{\text{ESG}}, \gamma_u^{\text{ESG}}]$ is very narrow. WBD and ASML illustrate that the s:n ratio can remain within 5% of s:n(0) for extended ranges of either $\gamma^{\text{ESG}} < 0$ or $\gamma^{\text{ESG}} > 0$. The results for AMD are representative of 13 of the 16 stocks for which $[\gamma_l^{\text{ESG}}, \gamma_u^{\text{ESG}}] \subset [-1, 1]$. For AMD and ASML, $Z_t^{(X)} > Z_t^{(\wedge \text{NDX})}$ (Figure 2) over the historical time period; as a consequence the ESG-adjusted price increases with γ^{ESG}. For WBD, $Z_t^{(\text{WBD})} < Z_t^{(\wedge \text{NDX})}$ and its ESG-adjusted stock price decreases as γ^{ESG} increases. PANW is the only stock of the 16 companies considered whose ESG score $Z_t^{(\text{PANW})}$ increased from below to above that of $\wedge$NDX. The $\gamma_l^{\text{ESG}} = -0.09$ and $\gamma_u^{\text{ESG}} = 0.09$ curves therefore cross each other near the start of 2022 (difficult to visualize in the plot for PANW in Figure 5).

Parameter fits

To compute option prices using the binomial BBSM model in Section 3, predictive empirical ESG-adjusted prices (equation(11)) were computed

assuming constant parameter values. Lindquist [5] (Section 9) suggested (but did not implement) procedures for fitting the parameters of a BBSM model. With minor modification, we follow their suggested procedure for estimating the risky-asset price parameters; we utilize a different procedure for estimating the riskless asset price parameters. The parameter values were estimated from the historical price data, as follows. Express the historical data as the trading dates $j = -M + 1, \ldots, -1, 0$ ($M = 2013$), where $j = -M + 1$ corresponds to 01/04/2016 and $j = 0$ to 01/02/2024. The date 01/02/2024 (i.e., $j = 0$) corresponds to the date for which option price data was collected and used in Section 5 to compute implied ESG affinity values.
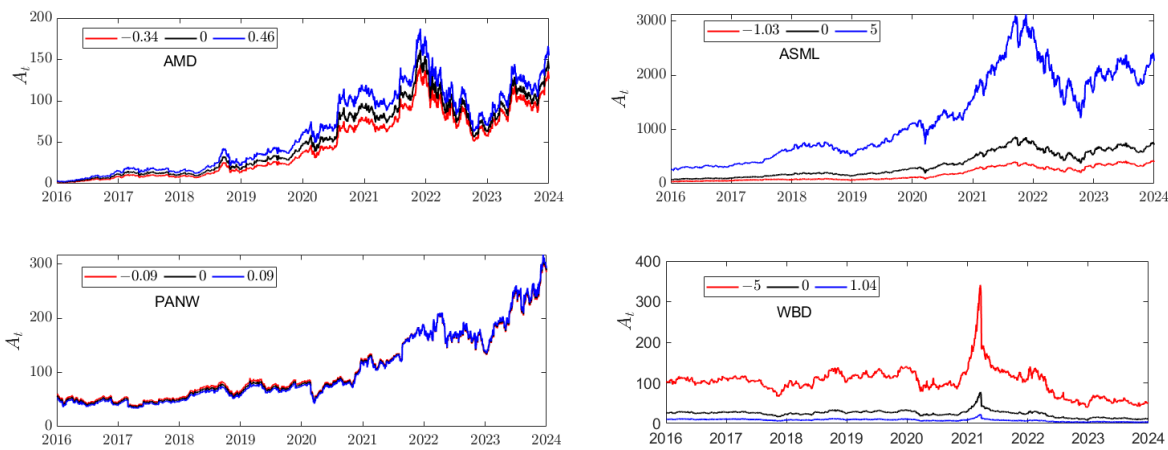
Figure 5. ESG-adjusted prices of selected stocks as γ^{ESG} varies over the set $\{\gamma_l^{\mathrm{ESG}}, 0, \gamma_h^{\mathrm{ESG}}\}$.

From equation (16) with constant coefficients, the conditional mean and variance of the discrete change in stock price are

$$
\begin{aligned}
E\left[c_{(k+1)\Delta,n} \,|\, \mathcal{F}_k^{(n)}\right] &= (a + \mu A_{k\Delta,n})\,\Delta, \\
\mathrm{Var}\left[c_{(k+1)\Delta,n} \,|\, \mathcal{F}_k^{(n)}\right] &= (v + \sigma A_{k\Delta,n})^2\,\Delta
\end{aligned}
\tag{35}
$$

The parameters a and μ were obtained using the regression

$$
\frac{c_{(j+1)\Delta,n}}{\Delta} = a + \mu A_{j\Delta,n} + \epsilon_{j\Delta,n}^{(1)}, \quad j = -M + 1, \ldots, -1
\tag{36}
$$

Using the approximation $(c_{(k+1)\Delta,n})^2 \approx \mathrm{Var}\left[c_{(k+1)\Delta,n} \,|\, \mathcal{F}_k^{(n)}\right]$, the parameters v and σ were estimated from the regression

$$
\frac{|c_{(j+1)\Delta,n}|}{\sqrt{\Delta}} = v + \sigma A_{j\Delta,n} + \epsilon_{j\Delta,n}^{(2)}, \qquad j = -M + 1, \ldots, -1
\tag{37}
$$

With constant parameters, the price dynamics (equation(13)) of the riskless asset has the discrete form

$$
\beta_{k\Delta,n} = \beta_{(k-1)\Delta,n} + \rho\Delta + r\Delta\beta_{(k-1)\Delta,n}
\tag{38}
$$

We note that the recursion relation (equation (38)) has the solution $\beta_{k\Delta,n} = (1 + r\Delta)^k \beta_0 + \rho\Delta \sum_{j=0}^{k-1}(1 + r\Delta)^j$. Under the limits $k \uparrow \infty$, $\Delta \downarrow 0$, such that $k\Delta = \tau$, where τ is a constant time, the limit of this discrete solution is $\beta_\tau =$

$e^{r\tau}\beta_0 + \rho/r[e^{r\tau} - 1]$, in agreement with the continuous solution to (equation (3)) under constant coefficients.

The parameters ρ and r were estimated from the regression

$$\frac{\beta_{(j+1)\Delta,n} - \beta_{j\Delta,n}}{\Delta} = \rho + r\beta_{j\Delta,n} + \delta_{j\Delta,n}, \qquad j = -M+1,\ldots,-1 \qquad (39)$$

The sequence of daily values $\beta_{j\Delta,n}$ required in equation (39) was generated as follows

$$\beta_{(j+1)\Delta,n} = (1 + r_{3,j}\Delta)\beta_{j\Delta,n}, \quad j = -M+1,\ldots,-1, \; \beta_{(-M+1)\Delta,n} = A_{(-M+1)\Delta,n} \quad (40)$$

where $r_{3,j}$ is the three-month U.S. Treasury bill rate, converted to a daily rate. In effect, equation (39) models the evolution of the yield of the three-month Treasury bill [41] (accessed 01/02/2024) using the discrete form (equation (38)) of the BBSM model riskless rate dynamics (equation (3)).

Finally, we estimated the probability p_n for the upward movement of the daily ESG-adjusted closing price by

$$p_n = \frac{1}{M-1} \sum_{j=-M+2}^{0} I_{c_{j\Delta,n>0}} \qquad (41)$$

where the indicator function $I_{x>0}$ satisfies $I_{x>0} = 1$ if $x > 0$ and $I_{x>0} = 0$ otherwise.

From equation (9), for each time t there exists a value $\gamma_{0,t}^{\text{ESG}} = -1/Z_t^{(X;I)} \in R$ such that $A_t = S_t^{(X)}\left(1 + \gamma_{0,t}^{\text{ESG}}Z_t^{(X;I)}\right) = 0$. Therefore if $Z_t^{(X;I)} = Z^{(X;I)}$, a time independent constant over the historical period for which the regression fits equations (36) and (37) are to be attempted, the linear regressions near the value $\gamma_0^{\text{ESG}} = -1/Z^{(X;I)}$ become ill-conditioned and unrealistic parameter fits result. As we utilized an eight-year historical window over which $Z_t^{(X;I)}$ had behaviors similar to that illustrated in Figure 3, this was not an issue.

Figure 6 shows the dependence of the values of the fitted parameters $\hat{a}$, $\hat{\mu}$, $\hat{\nu}$, $\hat{\sigma}$, $\hat{\rho}$, $\hat{r}$, $\hat{p}_n$ on $\gamma^{\text{ESG}} \in \left[\gamma_l^{\text{ESG}}, \gamma_u^{\text{ESG}}\right]$ for ASML and ROST. These are illustrative of the forms of dependence seen in the 16 stocks. In the plots for $\hat{p}_n$, the black curve indicates the value of p_n estimated using equation (41). A change in the value of $I_{c_{j\Delta,n}>0}$ by its smallest increment (± 1) as γ^{ESG} changes is visible as a corresponding jump in the value of $\hat{p}_n$. We used a Gaussian-weighted, moving average smoother (with a window of 21 days) to smooth the $\hat{p}_n$ values (red curve).

In equation (40) the value of γ^{ESG} only affects the value of $A_{(-M+1)\Delta,n}$. Consequently, in the fit equation (39) we see from Figure 6 that the parameter ρ depends on γ^{ESG}, while the parameter r is independent of the value γ^{ESG}. In fact the constant fitted value of $\hat{r}$ is independent of the stock considered, which makes sense as, except for an initial value $\beta_{(-M+1)\Delta,n} = A_{(-M+1)\Delta,n}$, equations (40) and (39) depend only on the riskless asset.
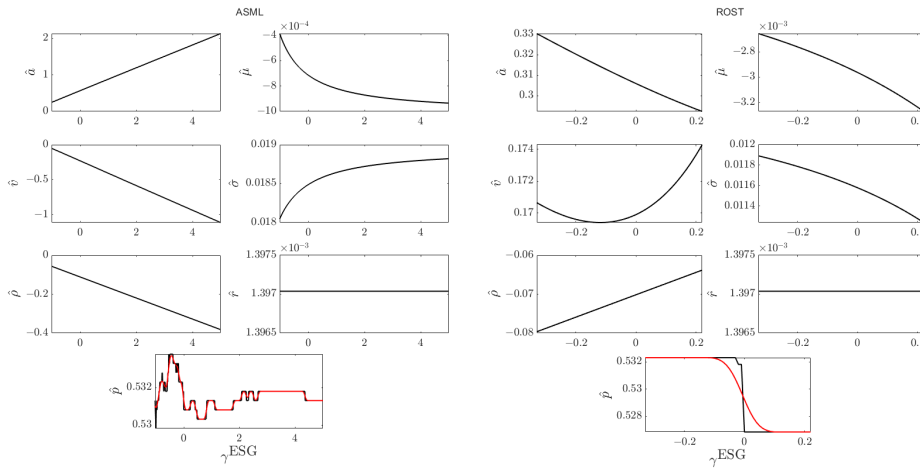
Figure 6. Parameter dependence on γ^{ESG} over their respective ranges $\left[\gamma_l^{ESG}, \gamma_u^{ESG}\right]$.
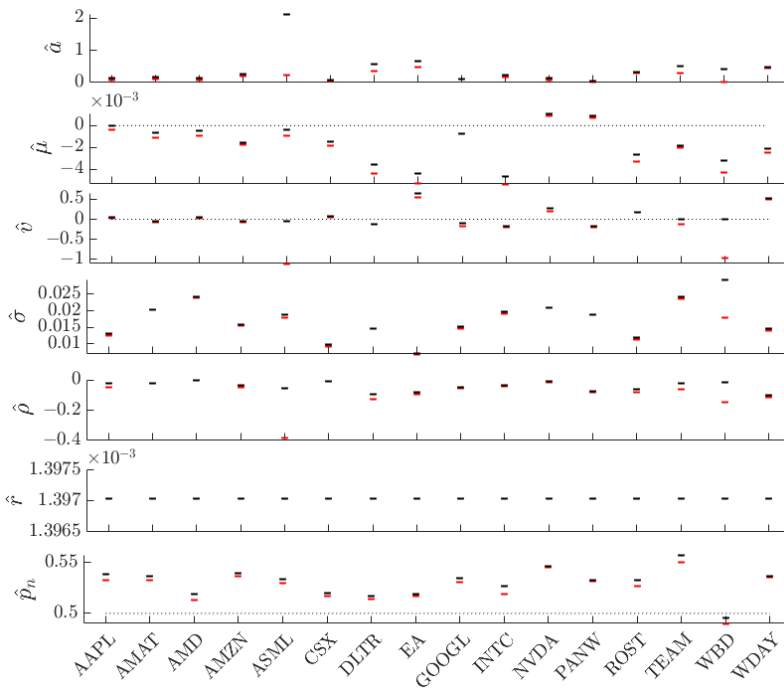
Figure 7. Range of fitted parameter values, by stock. The upper value of each range is black, the lower value is red. Dotted horizontal lines denote the value 0 or 0.5 as appropriate.

Figure 6 shows that, with the exception of $\hat{r}$, as γ^{ESG} varies over the range $\left[\gamma_l^{ESG}, \gamma_u^{ESG}\right]$, each fitted parameter varies over a range of values, with the range varying by stock. For each fitted parameter, Figure 7 compares, by stock, the range of values taken on by that parameter. Dotted horizontal lines are used to guide the eye to separate positive from negative parameter ranges, or, in the case of $\hat{p}_n$, to indicate stocks having $p_n > 0.5$. We note that the range $\left[\gamma_l^{ESG}, \gamma_u^{ESG}\right]$ for each stock includes $\gamma^{ESG} = 0$ (no ESG price adjustment). Even so, the MB parameters $\hat{a}$, $\hat{v}$ and $\hat{\rho}$ are consistently different from 0 over the full $\left[\gamma_l^{ESG}, \gamma_u^{ESG}\right]$ range (except for $\hat{v}$ for WBD). Thus the parameter fits, even for the financial stock price ($\gamma^{ESG} = 0$), show an admixture of MB and BSM behavior. The values of $\hat{a}$ and $\hat{\sigma}$ are positive

for all 16 stocks; for $\hat{\rho}$ all values are negative. For $\hat{\mu}$, all are negative except for two stocks, NVDA and PANW. Values of $\hat{v}$ are equally divided between positive and negative over the 16 stocks. Values of $\hat{p}_n$ exceed 0.5 for all stocks except WBD.

THE IMPLIED ESG AFFINITY

Let $C^{(\text{emp})}(A_0, T_i, K_j)$ denote published call option prices for an underlying stock having maturity date T_i, $i \in I$, and strike price K_j, $j \in J$. Let $C^{(\text{th})}\left(A_0, T_i, K_j; a, \mu, v, \sigma, \rho, r, p_n, \gamma^{\text{ESG}}\right)$ denote the call option price computed from Section 3 with constant parameters values. Let $\hat{\xi}$ denote the historical estimation of any parameter ξ. (Recall that, except for $\hat{r}$, the parameters have dependence on the value of γ^{ESG}.) Then implied values for γ^{ESG} are computed via

$$
\gamma^{(\text{ESG,imp})}(T_i, K_j)
$$

$$
= \underset{\gamma^{\text{ESG}}}{\arg\min} \left(\frac{C^{(\text{th})}\left(A_0, T_i, K_j; \hat{a}, \hat{\mu}, \hat{v}, \hat{\sigma}, \hat{\rho}, \hat{r}, \hat{p}_n, \gamma^{\text{ESG}}\right) - C^{(\text{emp})}(A_0, T_i, K_j)}{C^{(\text{emp})}(A_0, T_i, K_j)} \right)^2 \quad (42)
$$

Based upon call option prices published on 01/02/2024 [39], we computed theoretical call option prices for the same set of strike prices, K_j, $j \in J$, and maturity times T_i, $i \in I$. In equation (42), the parameters $\hat{a}, \hat{\mu}, \hat{v}, \hat{\sigma}, \hat{\rho}, \hat{p}_n$ used in the theoretical option computation were fit from the historical data for each value of γ^{ESG} tested in the minimization procedure. As the value of $\hat{r}$ is independent of the value of γ^{ESG} and of the stock, theoretically it only needed to be calculated once. However, it is computed from the same regression equation (39) that produces $\hat{\rho}$, so it was recomputed for each value of γ^{ESG} tested. The value $Z_t^{(X;^\wedge\text{NDX})}$ used to compute prices on the binomial tree was the smoothed value for 01/02/2024. The published call option prices for AAPL on 01/02/2024 are presented in Figure 8. In all plots, the maturity times T are presented in terms of trading days post 01/02/2024.

In contrast to some of the other stocks investigated, these option prices form a fairly "regular" surface over the published range of K_j, $j \in J^{(\text{AAPL})}$, and maturity times T_i, $i \in I^{(\text{AAPL})}$ values. The values $\gamma^{(\text{ESG,imp})}(T_i, K_j)$ computed from equation (42) are plotted as a surface in Figure 8. In preparing the final surface shown, triangulation-based nearest neighbor interpolation was used to fill in missing (T_i, K_j) values in the $\gamma^{(\text{ESG,imp})}$ surface. The surface was then smoothed using a Gaussian weighted, moving average algorithm. This smoothing produced relatively minor changes.

Analysis of the $\gamma^{(\text{ESG,imp})}$ surface is enhanced by consideration of surface contours as shown in the bottom left of the figure. The $\gamma^{(\text{ESG,imp})}(T, K) = 0$ contour lies between the contours –0.0833 and 0.229, indicating that option traders have a positive view (relative to ^NDX) of the ESG rating of AAPL in the upper left triangular region of out-of-the money (the adjusted closing price for AAPL on 01/02/2024 was \$185.64) strike prices and maturity dates not exceeding 110 trading days. However, over the majority of (T, K) values, the option traders have a negative view of the ESG rating of AAPL.
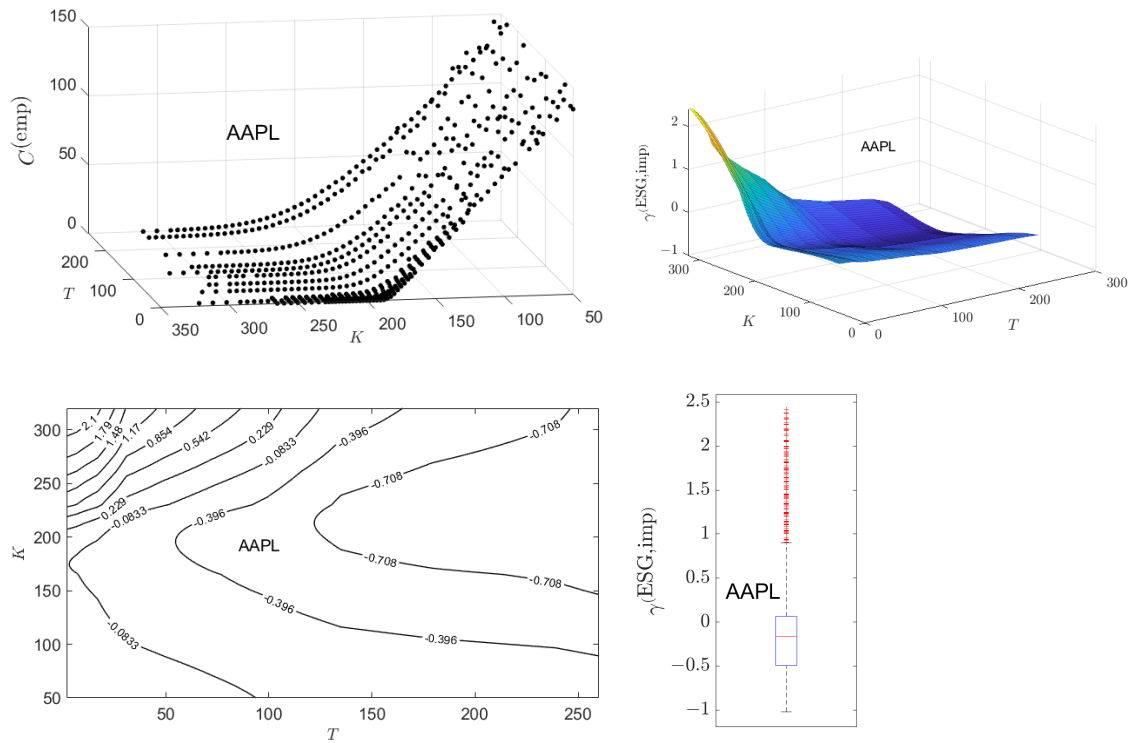
Figure 8. For the stock AAPL: (top left) The empirical option prices published for AAPL on 01/02/2024. (top right) The computed surface of $\gamma^{(\text{ESG,imp})}$ values. (bottom left) Contours of the $\gamma^{(\text{ESG,imp})}$ surface. (bottom right) Box-whisker summary of the distribution of $\gamma^{(\text{ESG,imp})}$ values.

A further view of the $\gamma^{(\text{ESG,imp})}$ values is presented in Figure 8 as a box-whisker summary of the distribution over the surface. Table A1 in Appendix presents the numerical values of the minimum, maximum, P_{25}, P_{50}, and P_{75} percentiles of the $\gamma^{(\text{ESG,imp})}$ distribution for AAPL. This table also presents the $\left[\gamma_l^{\text{ESG}}, \gamma_u^{\text{ESG}}\right]$ for AAPL based upon examination of historical adjusted ESG prices discussed in Section 4.3. The overwhelming majority of $\gamma^{(\text{ESG,imp})}$ values lie within the $\left[\gamma_l^{\text{ESG}}, \gamma_u^{\text{ESG}}\right]$ for AAPL, giving some confidence that the implied ESG affinity values being computed are consistent with semi-martingale behavior of the associated ESG-adjusted price.

To appreciate the implication of this, we define from equation (9) an implied ESG-adjusted price

$$A_t^{(\text{imp})} = S_t^{(X)} \left(1 + \gamma^{(\text{ESG,imp})} Z_t^{(X;\wedge\text{NDX})} \right) \tag{43}$$

where, for a given stock X, $\gamma^{(\text{ESG,imp})}$ is a value from the implied ESG affinity surface, and $Z_t^{(X;\wedge\text{NDX})}$ was the relative ESG score and $S_t^{(X)}$ the spot price price used in computing the surface. Figure 9 presents the surface of $A_t^{(\text{imp})}$ values computed from the $\gamma^{(\text{ESG,imp})}$ values of Figure 8. Also shown are contour levels of the $A_t^{(\text{imp})}$ corresponding to the analogous contour levels of $\gamma^{(\text{ESG,imp})}$ shown in Figure 8. Whether $A_t^{(\text{imp})}$ is larger or smaller than $S_t^{(X)}$ depends on the sign of the product $\gamma^{(\text{ESG,imp})} Z_t^{(X;\wedge\text{NDX})}$. If $Z_t^{(X;\wedge\text{NDX})}$ is positive, then positive values of $\gamma^{(\text{ESG,imp})}$ correspond to an ESG valuation that exceeds $S_t^{(X)}$. However, if $Z_t^{(X;\wedge\text{NDX})}$ is negative, then negative values of $\gamma^{(\text{ESG,imp})}$ correspond to an ESG valuation that exceeds

$S_t^{(X)}$. Thus, consideration of the $A_t^{(\text{imp})}$ surfaces rather than the $\gamma^{(\text{ESG,imp})}$ surfaces provides direct insight into the views of option traders on the ESG-valuation of stocks.
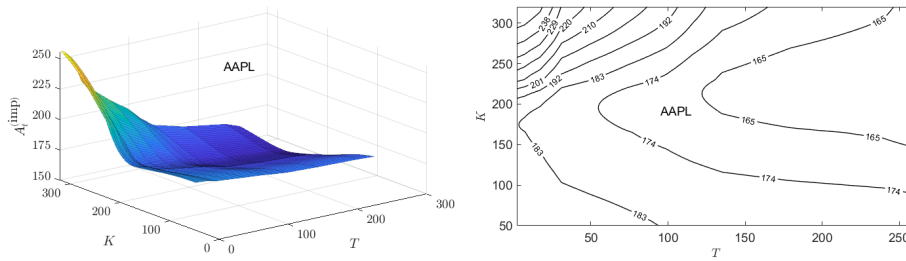
Figure 9. For the stock AAPL: (left) The computed surface of $A_t^{(\text{imp})}$ values. (right) Contours of the $A_t^{(\text{imp})}$ surface.

Since $Z_t^{(\text{AAPL},\wedge\text{NDX})}$ was positive on 01/02/2024, the surfaces of $\gamma^{(\text{ESG,imp})}$ and $A_t^{(\text{imp})}$ are identical except for a rescaling of the z-axis. Similarly the contour plots for $\gamma^{(\text{ESG,imp})}$ and $A_t^{(\text{imp})}$ are identical except for a rescaling of the value on the contour levels. The negative view of the option traders over most of the (T, K) range for AAPL, results in implied, ESG-adjusted prices for 01/02/2024 that correspondingly fall below the financial price of AAPL on 01/02/2024.

Figures B1 and B2 in Appendix B plot the published option prices on 01/02/2024 for all 16 stocks studied. The eight stocks for which $Z_t^{(X;\wedge\text{NDX})} > 0$ on $t = 01/02/2024$ are presented in Figure B1, while the eight stocks for which $Z_t^{(X;\wedge\text{NDX})} < 0$ are presented in Figure B2. This separation reflects the fact that when $Z_t^{(X;\wedge\text{NDX})} > 0$, the corresponding surfaces for $\gamma^{(\text{ESG,imp})}$ and $A_t^{(\text{imp})}$ will look like identical (rescaled) versions of each other. However, when $Z_t^{(X;\wedge\text{NDX})} < 0$, the surface $A_t^{(\text{imp})}$ will look like an inverted, rescaled version of the corresponding $\gamma^{(\text{ESG,imp})}$ surface. Examination of published option prices for PANW, TEAM, and WDAY show much greater irregularity over the range of K and T values than that shown for AAPL. This results in some corresponding surface irregularity (even after smoothing) in the $\gamma^{(\text{ESG,imp})}$ surface.

Plots of the $\gamma^{(\text{ESG,imp})}$ surfaces for all 16 stocks are presented in Figures C1 and C2 in Section C. The stock organization into two separate figures mirrors that for Figures B1 and B2. Figures C3 and C4 provide the contour plots of these surfaces. Box-whisker summaries of the distributions of $\gamma^{(\text{ESG,imp})}$ values are given in Figure C5. Plots of the $A_t^{(\text{imp})}$ surfaces for all 16 stocks are presented in Figures D1 and D2 in Section D. Figures D3 and D4 provide the contour plots of these surfaces.

To summarize the information in Appendices C and D, Figure 10 presents the box-whisker summaries of the distributions of $A_t^{(\text{imp})}$ values for each of the 16 stocks.

For ease of reference, the financial spot prices on 01/02/2024 are listed in Table A2. From the contour plots in Figures D3 and D4, one can then ascertain over what region of (T, K) values option traders view the ESG valuation of the stock to be higher than its financial price. For EA, INTC,

TEAM and WBD, spot traders have an implied ESG valuation that exceeds the spot price over most of the (T, K) region. For eight of the stocks (AAPL, AMAT, AMD, AMZN, ASML, CSX, NVDA, PANW), the implied ESG valuation exceeds the spot price over a triangular, out-of-the-money, shorter maturity time region as described above for AAPL. For the remaining four stocks, the implied ESG valuation exceeds the spot price over most of the out-of-the-money region. Thus, for 12 of the 16 stocks, option traders have in-the-money ESG valuations that are lower than the spot price.
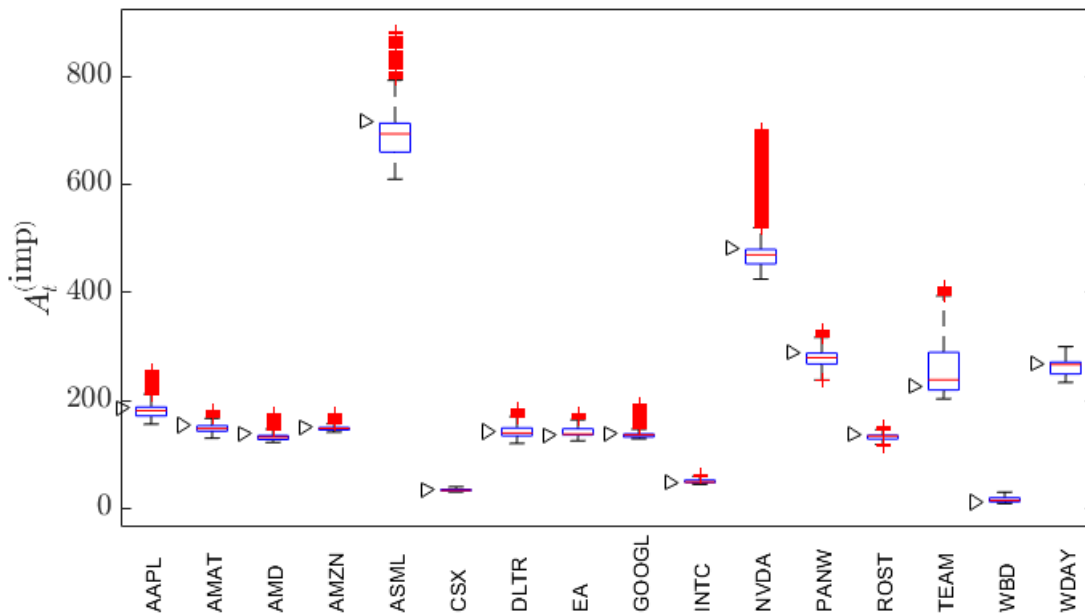
Figure 10. Box-whisker summaries of the distribution of $A_t^{(\text{imp})}$ values for all 16 stocks studied. The "right-arrow" to the left of each box-whisker plot for $A_t^{(\text{imp})}$ corresponds to the stock spot price on 01/02/2024.

TRADING FORWARD CONTRACTS UTILIZING INFORMATION ON ASSET PRICE DIRECTION

Hu [8] extended BSM-based binomial option pricing theory to complete markets containing traders that have information on the stock price direction. We further extend that theory using the BBSM-based binomial option pricing in complete markets of Section 3. For simplicity, we assume the parameters in the BBSM binomial model are constant: $a_{k\Delta,n} = a$, $\mu_{k\Delta,n} = \mu$, $\nu_{k\Delta,n} = \nu$, $\sigma_{k\Delta,n} = \sigma$, $\rho_{k\Delta,n} = \rho$, and $r_{k\Delta,n} = r$, $Z_{k\Delta,n}^{(X,I)} = Z^{(X,I)}$. As earlier, we continue to assume γ^{ESG} is constant.

Let $\aleph$ denote the trader (hedger) holding the short position in the option contract. Let $p_n^{\aleph} \in (0, 1)$ denote the probability that information held by $\aleph$ at time $k\Delta$, $k = 0, \ldots, n-1$, on the direction of stock price movement within any interval $[k\Delta, (k+1)\Delta]$ is correct. If $p_n^{\aleph} > 1/2$, $\aleph$ is an informed trader; if $p_n^{\aleph} < 1/2$, $\aleph$ is misinformed; and if $p_n^{\aleph} = 1/2$, we refer to $\aleph$ as a noisy trader. We assume $\aleph$'s informed trading actions do not influence market prices.

In [8], Shannon's entropy (see e.g.,[42,43]) is used to quantify the amount of information $\aleph$ possesses. As with the price movement probability p_n of Section 3, $p_n^{\aleph}$ is the probability governing a Bernoulli random variable

$\eta_{k,n}$ such that $P(\eta_{k,n} = 1) = 1 - P(\eta_{k,n} = 0) = p_n^{\aleph}$. Then Shannon's entropy is $H(p_n^{\aleph}) = -p_n^{\aleph} \ln p_n^{\aleph} - (1 - p_n^{\aleph}) \ln(1 - p_n^{\aleph})$, having maximum value $H(1/2) = \ln 2$. Hu [8] defined $\aleph$'s level of information as

$$\tau(p_n^{\aleph}) = \text{sign}(p_n^{\aleph} - 1/2) \frac{H(1/2) - H(p_n^{\aleph})}{H(p_n^{\aleph})} \tag{44}$$

where

$$\text{sign}(p_n^{\aleph} - 1/2) = \begin{cases} 1, & \text{if } 1/2 < p_n^{\aleph} \le 1, \\ 0, & \text{if } p_n^{\aleph} = 1/2, \\ -1, & \text{if } 0 \le p_n^{\aleph} < 1/2 \end{cases} \tag{45}$$

In [8], (44) is written in terms of the information distance

$$D(p_n^{\aleph}, 1/2) = H(1/2) - H(p_n^{\aleph}) = p_n^{\aleph} \ln(2p_n^{\aleph}) + (1 - p_n^{\aleph}) \ln(2(1 - p_n^{\aleph})) \tag{46}$$

We address the question of $\aleph$'s potential gain from trading with an information level $\tau(p_n^{\aleph}) > 0$. At any time $k\Delta$, $k = 0, \ldots, n-1$, $\aleph$ makes independent bets, $\eta_{k+1,n}$, $k = 0, \ldots, n-1$. Thus, the filtration equation (12) needs to be augmented with the sequence of $\aleph$'s independent bets

$$F^{(n;\aleph)} = \{\mathcal{F}_k^{(n,\aleph)} = \sigma(\zeta_{j,n}, \eta_{j,n} : j = 1, ..., k), \ \mathcal{F}_0^{(n,\aleph)} = \{\emptyset, \Omega\}\} \tag{47}$$

Specifically, relying on the information on stock-price direction, $\aleph$ adopts a trading strategy involving forward contracts. For convenience, we label the two scenarios given by equation (11) for the price of $\mathcal{A}$:

$$\begin{aligned} S_c^{(\text{up})} &: \zeta_{k+1,n} = 1, \text{resulting in} A_{(k+1)\Delta,n} = A_{k,n} + u_{k\Delta,n} w.p. p_n, \\ S_c^{(\text{down})} &: \zeta_{k+1,n} = 0, \text{resulting in} A_{(k+1)\Delta,n} = A_{k,n} + d_{k\Delta,n} w.p. 1 - p_n \end{aligned} \tag{48}$$

where $u_{k\Delta,n}$ and $d_{k\Delta,n}$ are given by equation (17) with constant coefficients. If at $k\Delta t$, $\aleph$ believes that $S_c^{(\text{up})}$ will happen, $\aleph$ takes a long position in $\Delta_{k\Delta}^{(\aleph)}$-forward contracts, for some $\Delta_{k\Delta}^{(\aleph)} >\in R_+$. The opposite party to this transaction is a noisy trader. An optimal value for $\Delta_{k\Delta}^{(\aleph)}$ is determined below. The forward contracts mature at $(k+1)\Delta$. If at $k\Delta$, $\aleph$ believes that $S_c^{(\text{down})}$ will happen, then $\aleph$ takes a short position in $\Delta_{k\Delta t}^{(\aleph)}$-forward contracts having maturity $(k+1)\Delta$.

Lindquist [5] developed the price of a forward contract under the BBSM model. Assuming there is no initial cost to enter into the forward contract and constant coefficients, the T-forward price of $\mathcal{A}$ is

$$F(t, T) = A_t \exp\left\{ \int_t^T \left(r + \frac{\rho}{\beta_s} \right) ds \right\} \tag{49}$$

where the constant coefficient solution to equation (3) is (see Equation (A3) of [5])

$$\beta_t = \begin{cases} (\beta_0 + \rho/r) e^{rt} - \rho/r & \text{if } r \neq 0, \\ \beta_0 + \rho t & \text{if } r = 0 \end{cases} \tag{50}$$

Evaluating equation (49) using equation (50) gives

$$F(t, T) = A_t \frac{\beta_T}{\beta_t} \tag{51}$$

Discretizing (51) over the time interval $k\Delta \to (k+1)\Delta$ and assuming $o(\Delta) = 0$, equation (51) becomes

$$
\begin{aligned}
F(k\Delta, (k+1)\Delta) &= A_{k\Delta}\frac{\beta_{(k+1)\Delta}}{\beta_{k\Delta}} \\
&= A_{k\Delta}\frac{(\beta_{k\Delta} + \rho/r)\,e^{r\Delta} - \rho/r}{\beta_{k\Delta}} \\
&= A_{k\Delta}(1 + [r + \rho/\beta_{k\Delta}]\Delta)
\end{aligned}
\tag{52}
$$

For notational brevity, define $r_{k\Delta} = r + \rho/\beta_{k\Delta}$.

Using equation (11), conditionally on $\mathcal{F}_k^{(n,\aleph)}$, the payoff possibilities of $\aleph$'s forward contract positions can be written as

$$
\begin{aligned}
P_{k\Delta \to (k+1)\Delta}^{(\aleph;\text{forward})} \mid \mathcal{F}_k^{(n,\aleph)} &= \Delta_{k\Delta}^{(\aleph)}
\begin{cases}
A_{(k+1)\Delta,n}^{(u)} - A_{k\Delta,n}(1 + r_{k\Delta}\Delta) & \text{w.p. } p_n p_n^{(\aleph)}, \\
A_{k\Delta,n}(1 + r_{k\Delta}\Delta) - A_{(k+1)\Delta,n}^{(d)} & \text{w.p. } (1-p_n)p_n^{(\aleph)}, \\
A_{k\Delta,n}(1 + r_{k\Delta}\Delta) - A_{(k+1)\Delta,n}^{(u)} & \text{w.p. } p_n\left(1 - p_n^{(\aleph)}\right), \\
A_{(k+1)\Delta,n}^{(d)} - A_{k\Delta,n}(1 + r_{k\Delta}\Delta) & \text{w.p. } (1-p_n)\left(1 - p_n^{(\aleph)}\right)
\end{cases} \\[2mm]
&= \Delta_{k\Delta}^{(\aleph)}
\begin{cases}
u_{k\Delta,n} - A_{k\Delta,n}r_{k\Delta}\Delta & \text{w.p. } p_n p_n^{(\aleph)}, \\
A_{k\Delta,n}r_{k\Delta}\Delta - d_{k\Delta,n} & \text{w.p. } (1-p_n)p_n^{(\aleph)}, \\
A_{k\Delta,n}r_{k\Delta}\Delta - u_{k\Delta,n} & \text{w.p. } p_n\left(1 - p_n^{(\aleph)}\right), \\
d_{k\Delta,n} - A_{k\Delta,n}r_{k\Delta}\Delta & \text{w.p. } (1-p_n)\left(1 - p_n^{(\aleph)}\right)
\end{cases}
\end{aligned}
\tag{53}
$$

The conditional expected payoff is

$$
\begin{aligned}
&E\left[P_{k\Delta \to (k+1)\Delta}^{(\aleph;\text{forward})} \mid \mathcal{F}_k^{(n,\aleph)}\right] \\
&= \Delta_{k\Delta}^{(\aleph)}\left(2p_n^{\aleph} - 1\right)\left[p_n u_{k\Delta,n} - (1-p_n)d_{k\Delta,n} + (1-2p_n)A_{k,n}r_{k\Delta}\Delta\right]
\end{aligned}
\tag{54}
$$

with $u_{k\Delta,n}$ and $d_{k\Delta,n}$ given by equation (17).

We write

$$
p_n^{\aleph} = \frac{(1 + \lambda_\Delta^{(\aleph)}\sqrt{\Delta})}{2}
\tag{55}
$$

where, $0 < \lambda_\Delta^{(\aleph)}\sqrt{\Delta} \le 1$, for any finite value of Δ. $\lambda_\Delta^{(\aleph)}$ is referred to as $\aleph$'s information intensity. Again assuming $o(\Delta) = 0$,

$$
E\left[P_{k\Delta \to (k+1)\Delta}^{(\aleph;\text{forward})} \mid \mathcal{F}_k^{(n,\aleph)}\right] = 2\sqrt{p_n(1-p_n)}\,\lambda_\Delta^{(\aleph)}\Delta_{k\Delta}^{(\aleph)}\psi_{k\Delta,n}\Delta
\tag{56}
$$

It is sufficient to require terms of $o(\Delta)$ to vanish in order to apply invariance principles, such as that by Donsker and Prokhorov, to obtain the continuum limits of this discrete formulation.

Under the same assumption, the conditional variance of $\aleph$'s payoff is

$$
\text{Var}\left[P_{k\Delta \to (k+1)\Delta}^{(\aleph;\text{forward})} \mid \mathcal{F}_k^{(n,\aleph)}\right] = \left(\Delta_{k\Delta}^{(\aleph)}\psi_{k\Delta,n}\right)^2 \Delta
\tag{57}
$$

The instantaneous information ratio is then

$$
IR\left(P_{k\Delta \to (k+1)\Delta}^{(\aleph;\text{forward})} \mid \mathcal{F}_k^{(n,\aleph)}\right) = \frac{E\left[P_{k\Delta \to (k+1)\Delta}^{(\aleph;\text{forward})} \mid \mathcal{F}_k^{(n,\aleph)}\right]}{\sqrt{\text{Var}\left[P_{k\Delta \to (k+1)\Delta}^{(\aleph;\text{forward})} \mid \mathcal{F}_k^{(n,\aleph)}\right]\Delta}} = 2\sqrt{p_n(1-p_n)}\lambda_\Delta^{(\aleph)}
\tag{58}
$$

As $\lambda_\Delta^{(\aleph)}$ is positive, the information ratio on the payoff of $\aleph$'s strategy increases: as $\aleph$'s information intensity increases, and when $p_n \to 1/2$.

Expressed differently, when $p_n \downarrow 0$ or $p_n \uparrow 1$, the price movement becomes obvious to all traders and $\aleph$ can therefore be "no more informed" than a noisy trader.

To hedge the short position in the option, $\aleph$ executes the positions equation (19), while simultaneously running the futures trading strategy. This leads to an enhanced price process for $\aleph$, the dynamics of which can be expressed as

$$
A^{(\aleph)}_{(k+1)\Delta,n} = \begin{cases}
A^{(u)}_{(k+1)\Delta,n} + \Delta^{(\aleph)}_{k\Delta}\left(A^{(u)}_{(k+1)\Delta,n} - A_{k\Delta,n}(1 + r_{k\Delta}\Delta)\right) & \text{w.p. } p_n p^{(\aleph)}_n, \\
A^{(d)}_{(k+1)\Delta,n} + \Delta^{(\aleph)}_{k\Delta}\left(A_{k\Delta,n}(1 + r_{k\Delta}\Delta) - A^{(d)}_{(k+1)\Delta,n}\right) & \text{w.p. } (1 - p_n)p^{(\aleph)}_n, \\
A^{(u)}_{(k+1)\Delta,n} + \Delta^{(\aleph)}_{k\Delta}\left(A_{k\Delta,n}(1 + r_{k\Delta}\Delta) - A^{(u)}_{(k+1)\Delta,n}\right) & \text{w.p. } p_n\left(1 - p^{(\aleph)}_n\right), \\
A^{(d)}_{(k+1)\Delta,n} + \Delta^{(\aleph)}_{k\Delta}\left(A^{(d)}_{(k+1)\Delta,n} - A_{k\Delta,n}(1 + r_{k\Delta}\Delta)\right) & \text{w.p. } (1 - p_n)\left(1 - p^{(\aleph)}_n\right)
\end{cases}
$$
(59)

$k = 0, 1, \ldots, n - 1$, $n\Delta = T$. The price change of the process (59) is

$$
c^{(\aleph)}_{(k+1)\Delta,n} = A^{(\aleph)}_{(k+1)\Delta,n} - A_{k\Delta,n}, \qquad k = 0, \ldots, n - 1, \quad c^{(\aleph)}_{0,n} = 0
$$
(60)

Conditionally on $\mathcal{F}^{(n,\aleph)}_k$, and using equation (17),

$$
\begin{aligned}
E\left[c^{(\aleph)}_{k+1\Delta,n} \,\middle|\, \mathcal{F}^{(n,\aleph)}_k\right] &= \varphi_{k\Delta,n}\Delta + \Delta^{(\aleph)}_{k\Delta}\lambda^{(\aleph)}_\Delta\sqrt{p_n(1 - p_n)}\,\psi_{k\Delta,n}\Delta\,, \\
\text{Var}\left[c^{(\aleph)}_{k+1\Delta,n} \,\middle|\, \mathcal{F}^{(n,\aleph)}_k\right] &= \left(1 + \left(\Delta^{(\aleph)}_{k\Delta}\right)^2\right)\psi^2_{k\Delta,n}\Delta
\end{aligned}
$$
(61)

It is in $\aleph$'s interest to find the value of $\Delta^{(\aleph)}_{k\Delta}$ which maximizes the conditional Markowitz' expected utility function,

$$
U\left(c^{(\aleph)}_{(k+1)\Delta,n} \,\middle|\, \mathcal{F}^{(n,\aleph)}_k\right) = E\left[c^{(\aleph)}_{(k+1)\Delta,n} \,\middle|\, \mathcal{F}^{(n,\aleph)}_k\right] - \alpha^{(\aleph)}\,\text{Var}\left[c^{(\aleph)}_{(k+1)\Delta,n} \,\middle|\, \mathcal{F}^{(n,\aleph)}_k\right]
$$
(62)

where $\alpha^{(\aleph)} \geq 0$ is $\aleph$'s risk-aversion parameter. Using equation (61), $U\left(c^{(\aleph)}_{(k+1)\Delta,n} \,\middle|\, \mathcal{F}^{(n,\aleph)}_k\right)$ is maximized for

$$
\Delta^{(\aleph,\text{opt})}_{k\Delta t} = \frac{\sqrt{p_n(1 - p_n)}\,\lambda^{(\aleph)}_\Delta}{2\alpha^{(\aleph)}\psi_{k\Delta,n}}
$$
(63)

Under the optimal value,

$$
\begin{aligned}
E\left[c^{(\aleph)}_{(k+1)\Delta,n} \,\middle|\, \mathcal{F}^{(n,\aleph)}_k\right] &= \varphi_{k\Delta,n}\Delta + \frac{p_n(1 - p_n)}{2\alpha^{(\aleph)}}\left(\lambda^{(\aleph)}_\Delta\right)^2\Delta, \\
\text{Var}\left[c^{(\aleph)}_{(k+1)\Delta,n} \,\middle|\, \mathcal{F}^{(n,\aleph)}_k\right] &= [H(\aleph)\psi_{k\Delta,n}]^2\Delta, \\
H(\aleph) &= \sqrt{1 + p_n(1 - p_n)\left[\frac{\lambda^{(\aleph)}_\Delta}{2\alpha^{(\aleph)}\psi_{k\Delta,n}}\right]^2}
\end{aligned}
$$
(64)

and the instantaneous conditional market price of risk for $\aleph$ is

$$
\begin{aligned}
\Phi\left(c^{(\aleph)}_{(k+1)\Delta,n} \,\middle|\, \mathcal{F}^{(n,\aleph)}_k\right) &= \frac{E\left[c^{(\aleph)}_{(k+1)\Delta,n} \,\middle|\, \mathcal{F}^{(n,\aleph)}_k\right] - \chi_{k\Delta,n}\Delta}{\sqrt{\text{Var}\left[c^{(\aleph)}_{(k+1)\Delta,n} \,\middle|\, \mathcal{F}^{(n,\aleph)}_k\right]\Delta}} \\
&= \frac{\varphi_{k\Delta,n} - \chi_{k\Delta,n} + \left(\lambda^{(\aleph)}_\Delta\right)^2 p_n(1 - p_n)/(2\alpha^{(\aleph)})}{H(\aleph)\psi_{k\Delta,n}}
\end{aligned}
$$
(65)

If $\aleph$ had not traded futures on the information possessed, the trader's instantaneous conditional market price of risk would have been the same as a noisy trader

$$\Phi\left(c_{(k+1)\Delta,n} \mid \mathcal{F}_k^{(n)}\right) = \frac{E\left[c_{(k+1)\Delta,n} \mid \mathcal{F}_k^{(n)}\right] - \chi_{k\Delta,n}\Delta}{\sqrt{\mathrm{Var}\left[c_{(k+1)\Delta,n} \mid \mathcal{F}_k^{(n)}\right]\Delta}} = \frac{\varphi_{k\Delta,n} - \chi_{k\Delta,n}}{\psi_{k\Delta,n}} \tag{66}$$

Thus, $\aleph's$ futures trading results in an (optimized) dividend $D_{k\Delta}^{\aleph}$ yield over the time interval $[k\Delta, (k+1)\Delta)$ determined by the solution of

$$\frac{\varphi_{k\Delta,n} + D_{k\Delta}^{\aleph} - \chi_{k\Delta,n}}{\psi_{k\Delta,n}} = \Phi\left(c_{(k+1)\Delta,n}^{(\aleph)} \mid \mathcal{F}_k^{(n,\aleph)}\right) \tag{67}$$

Thus,

$$D_{k\Delta t}^{\aleph} = (\varphi_{k\Delta,n} - \chi_{k\Delta,n})\left[\frac{1}{H(\aleph)} - 1\right] + \frac{p_n(1-p_n)\lambda_{\Delta}^{(\aleph)2}}{2\alpha^{(\aleph)}H(\aleph)} \tag{68}$$

We note that, relative to a noisy trader,

$$\mathrm{Var}\left[c_{(k+1)\Delta,n}^{(\aleph)} \mid \mathcal{F}_k^{(n,\aleph)}\right] = [H(\aleph)]^2\psi_{k\Delta,n}^2\Delta \geq \psi_{k\Delta,n}^2\Delta = \mathrm{Var}\left[c_{(k+1)\Delta,n} \mid \mathcal{F}_k^{(n)}\right] \tag{69}$$

Equality between the first and last terms in equation (69) is obtained for $p_n = 0$ or $p_n = 1$ since, under these limits, all traders become aware of the direction of the price movement.

We investigate the dividend payout $D_{k\Delta t}^{\aleph}$ as a function of $\lambda_{\Delta}^{(\aleph)}$ and $\alpha^{(\aleph)}$. From equation (64) we note that $H(\aleph)$ is a monotonic function of $\lambda_{\Delta}^{(\aleph)}/\alpha^{(\aleph)}$ having the limits $H(\aleph) = 1$ and $H(\aleph) = \left[\sqrt{p_n(1-p_n)}/(2\psi_{k\Delta,n})\right](\lambda_{\Delta}^{(\aleph)}/\alpha^{(\aleph)})$. Under the limit $H(\aleph) = 1$, which corresponds to sufficiently small values of $\lambda_{\Delta}^{(\aleph)}$ or sufficiently large values of $\alpha^{(\aleph)}$,

$$D_{k\Delta t}^{\aleph} = \frac{p_n(1-p_n)\lambda_{\Delta}^{(\aleph)2}}{2\alpha^{(\aleph)}} \tag{70}$$

which is always positive, increasing with $\lambda_{\Delta}^{(\aleph)}$ and decreasing as $\alpha^{(\aleph)}$ increases. Under the limit $H(\aleph) = \left[\sqrt{p_n(1-p_n)}/(2\psi_{k\Delta,n})\right](\lambda_{\Delta}^{(\aleph)}/\alpha^{(\aleph)})$, which corresponds to sufficiently large values of $\lambda_{\Delta}^{(\aleph)}$ or sufficiently small values of $\alpha^{(\aleph)}$,

$$\begin{aligned} D_{k\Delta t}^{\aleph} &= (\varphi_{k\Delta,n} - \chi_{k\Delta,n})\left[\frac{\alpha^{(\aleph)}}{\lambda_{\Delta}^{(\aleph)}}\frac{2\psi_{k\Delta,n}}{\sqrt{p_n(1-p_n)}} - 1\right] + \sqrt{p_n(1-p_n)}\lambda_{\Delta}^{(\aleph)}\psi_{k\Delta,n} \\ &\approx \sqrt{p_n(1-p_n)}\lambda_{\Delta}^{(\aleph)}\psi_{k\Delta,n} - (\varphi_{k\Delta,n} - \chi_{k\Delta,n}) \end{aligned} \tag{71}$$

In this limit, the dividend payout is essentially independent of $\alpha^{(\aleph)}$.

CONCLUSION

Dynamic asset pricing based upon geometric Brownian motion [2,3] has had a tremendous' impact on finance theory. While having had difficulty gaining acceptance, dynamic pricing based upon arithmetic Brownian motion [1] has certain attractive features. The unified BBSM model of [5] encompasses the strengths of both models. By adapting the BBSM

framework to a model of ESG-adjusted asset valuation, we put the full strength of the BBSM model to practical use. Using an empirical data set of 16 stocks taken from the Nasdaq-100, based on call option prices for 01/02/2024 we have shown that, generally, option traders were implying ESG-adjusted prices that exceed the spot price in the out-of-the-money region, while in-the-money, ESG-adjusted prices were lower that the spot price. A follow-up study is required to determine how universal an observation this may be. It would be interesting to investigate call option prices issued during periods of bull and bear markets, and during market disruptions.

We have further extended this ESG-BBSM model to consider futures trading strategy accessible to a trader $\aleph$ holding information on the direction of ESG-adjusted prices. It would be of interest to evaluate $\aleph$'s optimal dividend payout by, for example, projecting it forward on the binomial tree and computing an expected dividend at time $t + T$. While this could be evaluated for a specific asset, using historical estimated values $\hat{a}$, $\hat{\mu}$, $\hat{v}$, $\hat{\sigma}$, $\hat{\rho}$, $\hat{r}$, $\hat{Z}^{X;I}$, and a spot price S_t (with $\beta_t = S_t$), there is no historical information available for γ^{ESG}, while the parameters $\lambda_\Delta^{(\aleph)}$ and $\alpha^{(\aleph)}$ are trader-dependent. Thus, estimates of an expected dividend payout at $t + T$ require an investigation of a three dimensional phase space - a fairly daunting prospect best left for a separate study.

DATA AVAILABILITY

The dataset of the study is available from the authors upon request from corresponding author.

AUTHOR CONTRIBUTIONS

Conceptualization, STR, WBL; Methodology, WBL, NAN, BD, AS; Formal Analysis, WBL, NAN, BD, PY, AS, STR, FJF; Investigation, WBL, NAN, BD, PY, AS, STR, FJF; Writing—Original Draft Preparation, NAN, AS, BD, PY; Writing—Review and Editing, WBL, NAN, BD, PY, AS, STR, FJF; Supervision, STR, WBL. All authors have read and agreed to the published version of the manuscript.

CONFLICTS OF INTEREST

The authors declare no conflict of interest.

APPENDICES

Appendix A. Tables

Table A1. Historical $[\gamma_l^{\text{ESG}}, \gamma_u^{\text{ESG}}]$ range and option price $\gamma^{(\text{ESG,imp})}$ distribution summary statistics.

Ticker	$[\gamma_l^{\text{ESG}}, \gamma_u^{\text{ESG}}]$	Min	P_{25}	P_{50}	P_{75}	Max
AAPL	[−1.16, 2.05]	−1.02	−0.49	−0.16	−0.06	2.42
AMAT	[−0.26, 0.32]	−0.50	−0.23	−0.13	−0.03	0.58
AMD	[−0.34, 0.46]	−0.46	−0.32	−0.18	−0.10	1.03
AMZN	[−0.36, 0.33]	−1.04	−0.00	0.07	0.19	0.36
ASML	[−1.03, 5.00]	−0.35	−0.18	−0.08	−0.01	0.53
CSX	[−0.43, 0.52]	−0.45	−0.25	−0.09	0.10	0.60
DLTR	[−0.37, 0.29]	−0.79	−0.12	0.05	0.14	0.42
EA	[−0.17, 0.15]	−0.89	−0.27	−0.04	−0.01	0.24
GOOGL	[−0.72, 0.63]	−2.97	0.00	0.12	0.31	0.50
INTC	[−0.13, 0.19]	−0.30	0.00	0.11	0.49	1.45
NVDA	[−0.42, 0.58]	−0.36	−0.18	−0.08	−0.01	1.39
PANW	[−0.09, 0.09]	−1.36	−0.56	−0.25	−0.04	1.08
ROST	[−0.33, 0.22]	−0.18	0.02	0.04	0.11	0.26
TEAM	[−0.78, 0.50]	−1.94	−0.67	−0.12	0.08	0.25
WBD	[−5.00, 1.04]	−2.33	−1.06	−0.42	−0.08	0.30
WDAY	[−0.55, 0.45]	−0.66	−0.05	0.04	0.41	0.74

Table A2. Adjusted closing prices on 01/02/2024 for the 16 stocks studied.

Ticker	Price (USD)
AAPL	185.64
AMAT	154.37
AMD	138.58
AMZN	149.93
ASML	716.92
CSX	34.62
DLTR	142.54
EA	135.78
GOOGL	138.17
INTC	47.80
NVDA	481.68
PANW	288.92
ROST	137.68
TEAM	226.67
WBD	11.66
WDAY	268.28

Appendix B. Plots of empirical option data $C^{(\mathbf{emp})}$

Figure B1 plots the empirical call option contract prices $C^{(\mathrm{emp})}$ as a function of strike price K and time to maturity T for the eight companies for which $Z_t^{(X,\wedge\mathrm{NDX})} > 0$ for t = 01/02/2024 while Figure B2 plots the same for the eight companies for which $Z_t^{(X,\wedge\mathrm{NDX})} < 0$ for t = 01/02/2024.
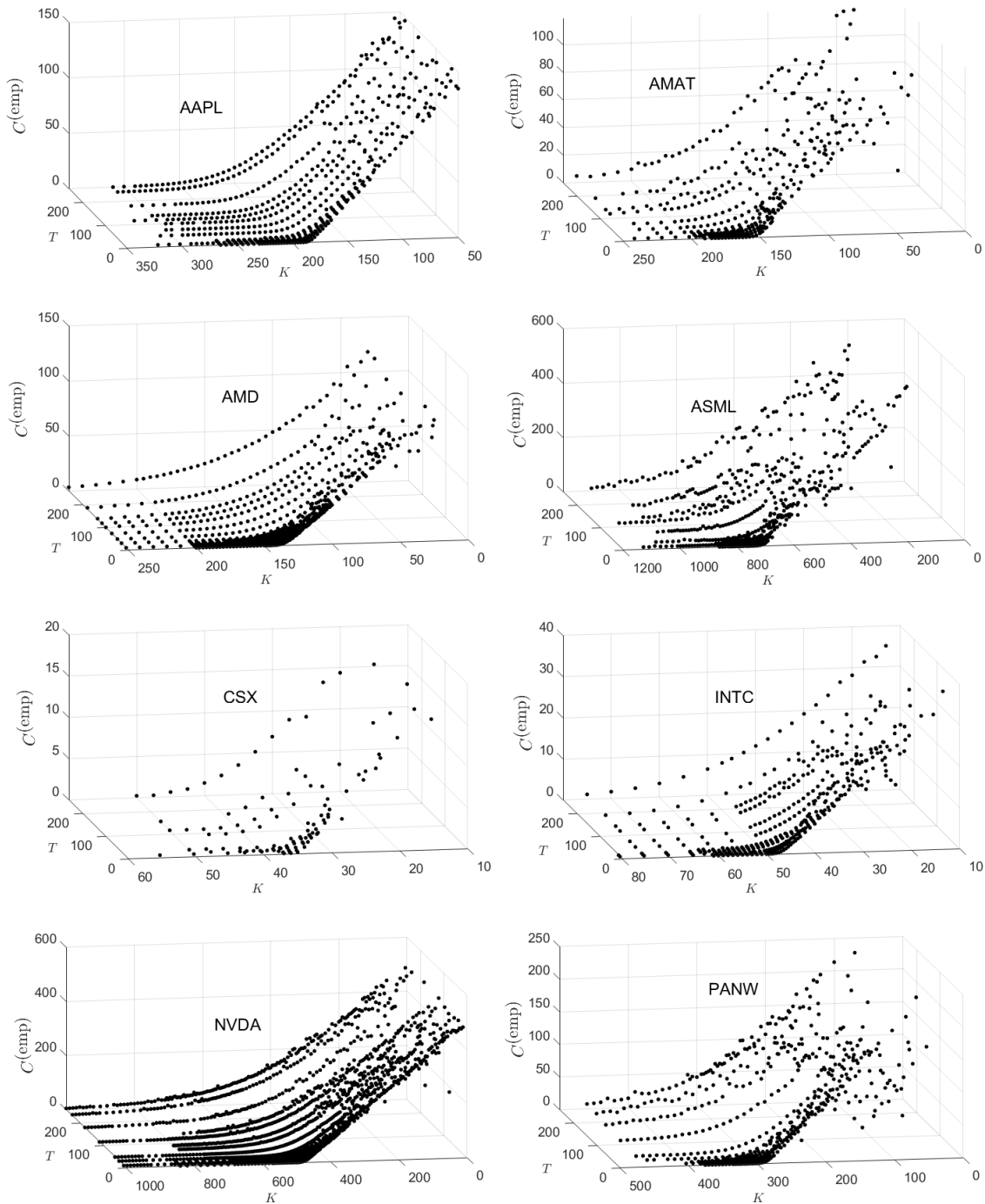
Figure B1. Empirical option prices $C^{(\mathrm{emp})}$ for the indicated stocks with $Z_t^{(X;\wedge\mathrm{NDX})} > 0$ on t = 01/02/2024.
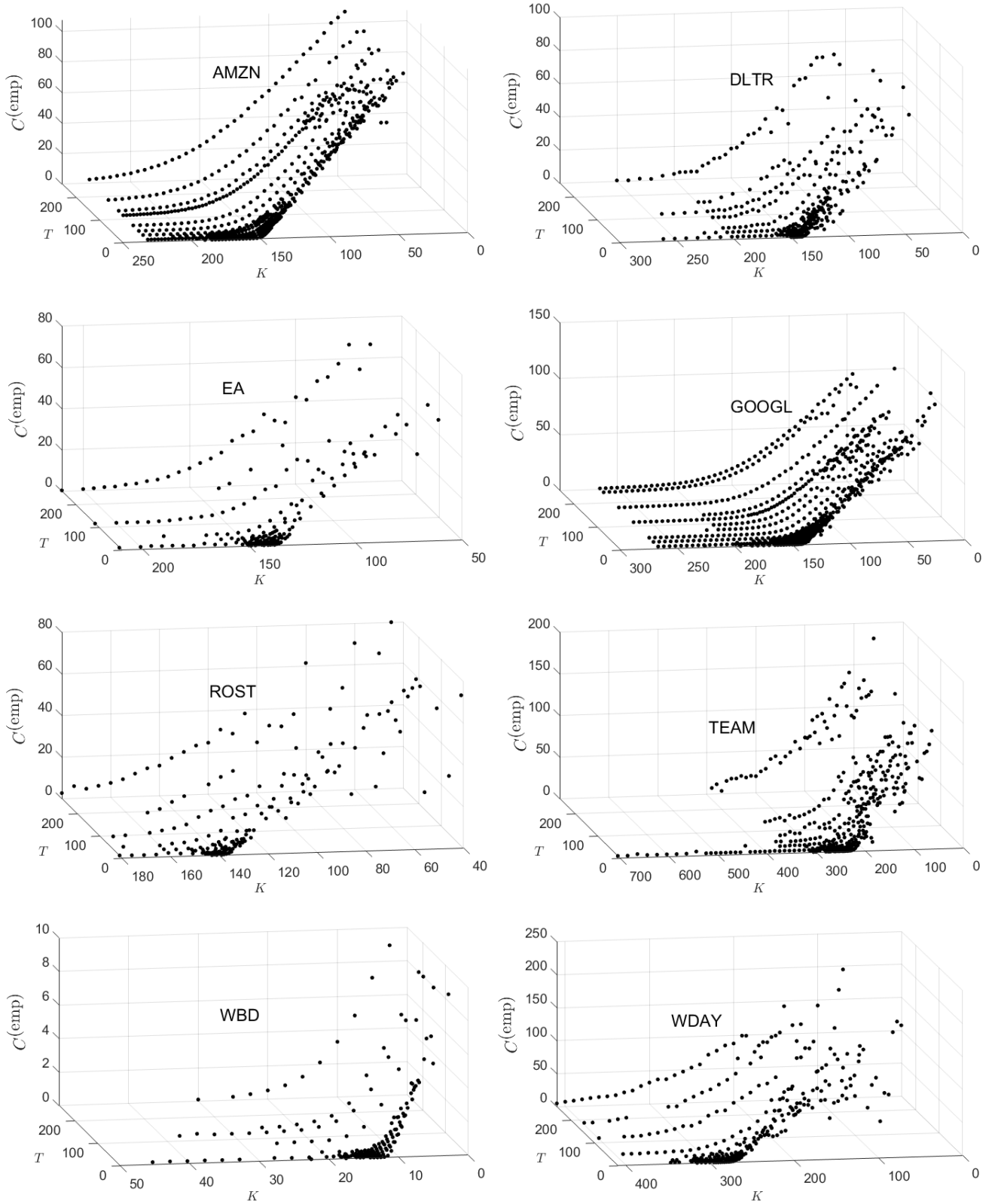
Figure B2. Empirical option prices $C^{(\text{emp})}$ for the indicated stocks with $Z_t^{(X,\wedge\text{NDX})} < 0$ on t = 01/02/2024.

Appendix C. Plots of $\gamma^{(\text{ESG,imp})}$

Figure C1 plots $\gamma^{(\text{ESG,imp})}$ as a function of strike price K and time to maturity T for the eight companies for which $Z_t^{(X,\wedge\text{NDX})} > 0$ on $t = 01/02/2024$.
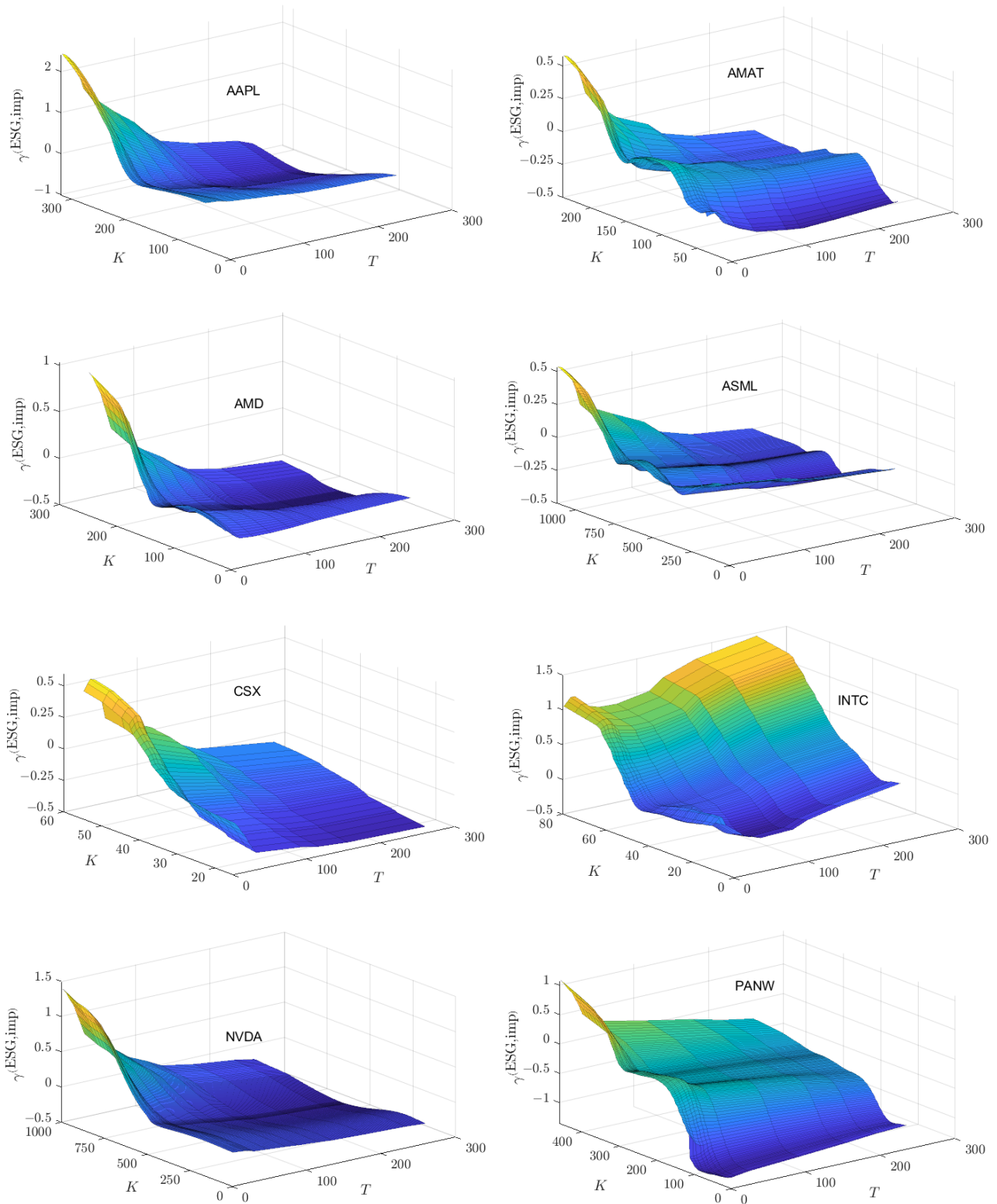
Figure C1. Implied surfaces $\gamma^{(\text{ESG,imp})}$ for the indicated stocks with $Z_t^{(X;\wedge\text{NDX})} > 0$ on $t = 01/02/2024$.
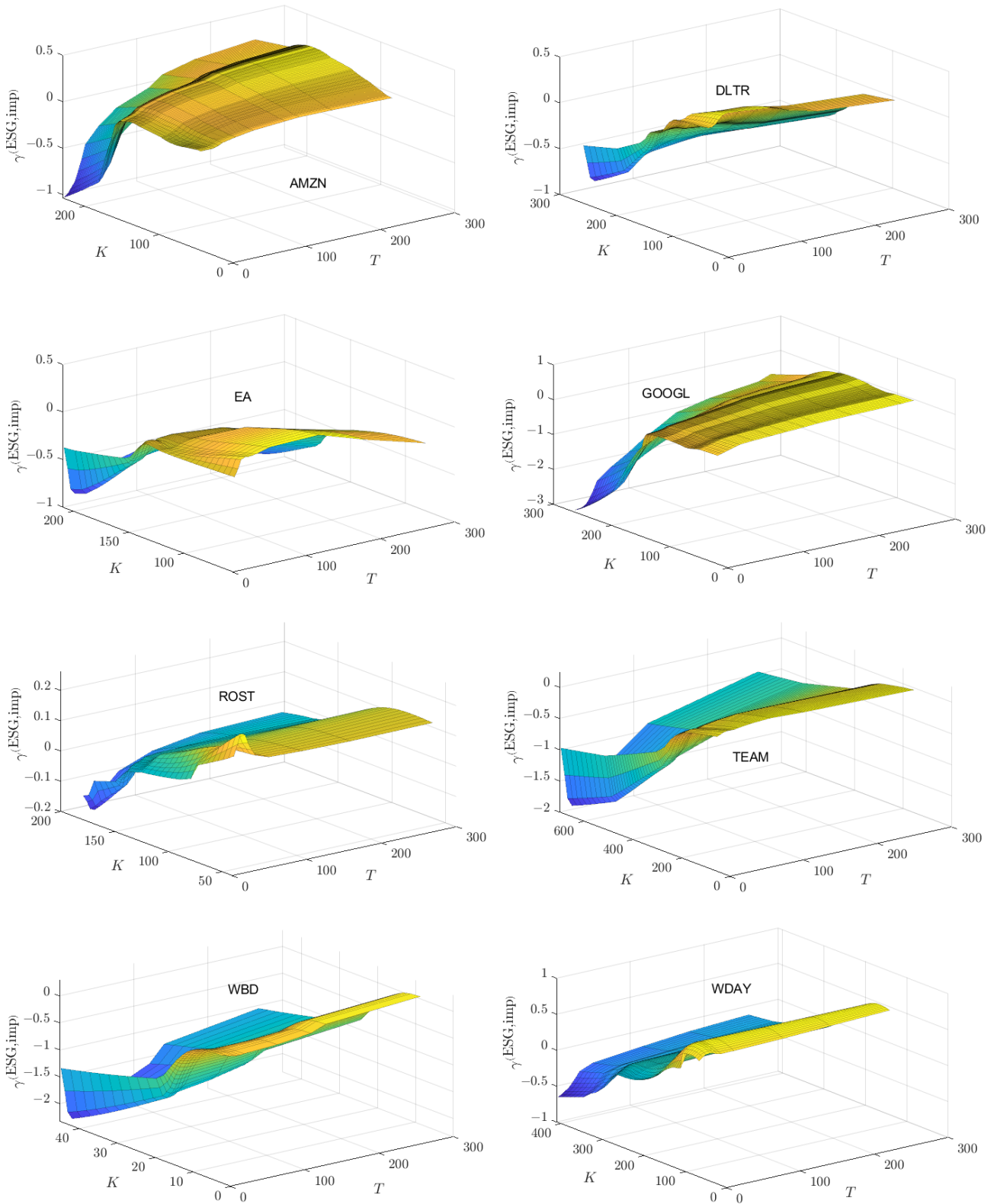
Figure C2. Implied surfaces $\gamma^{(\text{ESG,imp})}$ for the indicated stocks with $Z_t^{(X,^\wedge\text{NDX})} < 0$ on t = 01/02/2024.

Figure C2 plots $\gamma^{(\text{ESG,imp})}$ for the eight companies for which $Z_t^{(X,^\wedge\text{NDX})} < 0$ on t = 01/02/2024.
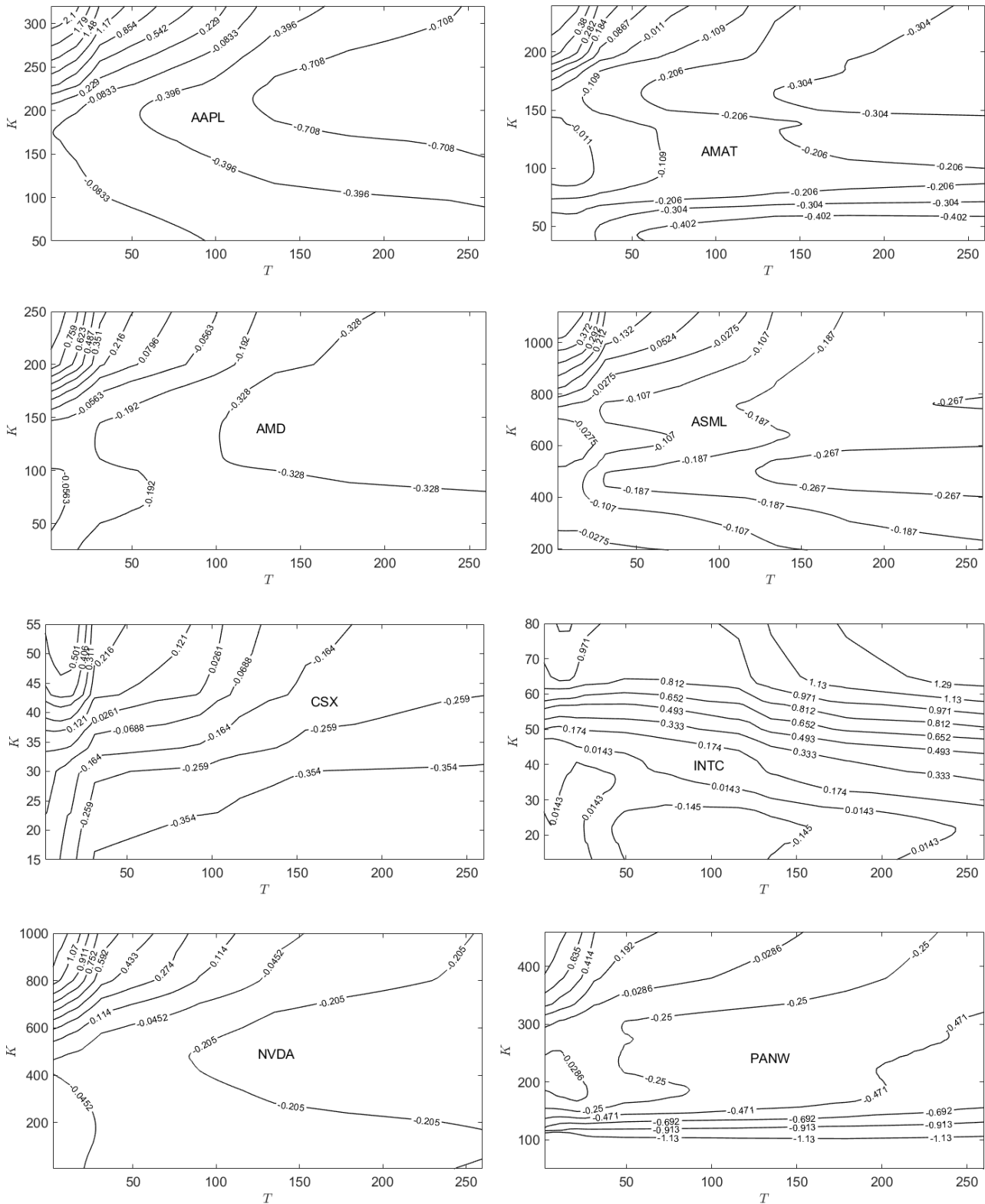
Figure C3. Contours of $\gamma^{(\mathrm{ESG,imp})}$ for the indicated stocks with $Z_t^{(X;\wedge\mathrm{NDX})} > 0$ on t = 01/02/2024.

Figure C3 plots contours of $\gamma^{(\mathrm{ESG,imp})}$ as a function of strike price K and time to maturity T for the eight companies for which $Z_t^{(X,\wedge\mathrm{NDX})} > 0$ for t = 01/02/2024, while Figure C4 plots the same for the eight companies for which $Z_t^{(X,\wedge\mathrm{NDX})} < 0$ for t = 01/02/2024.
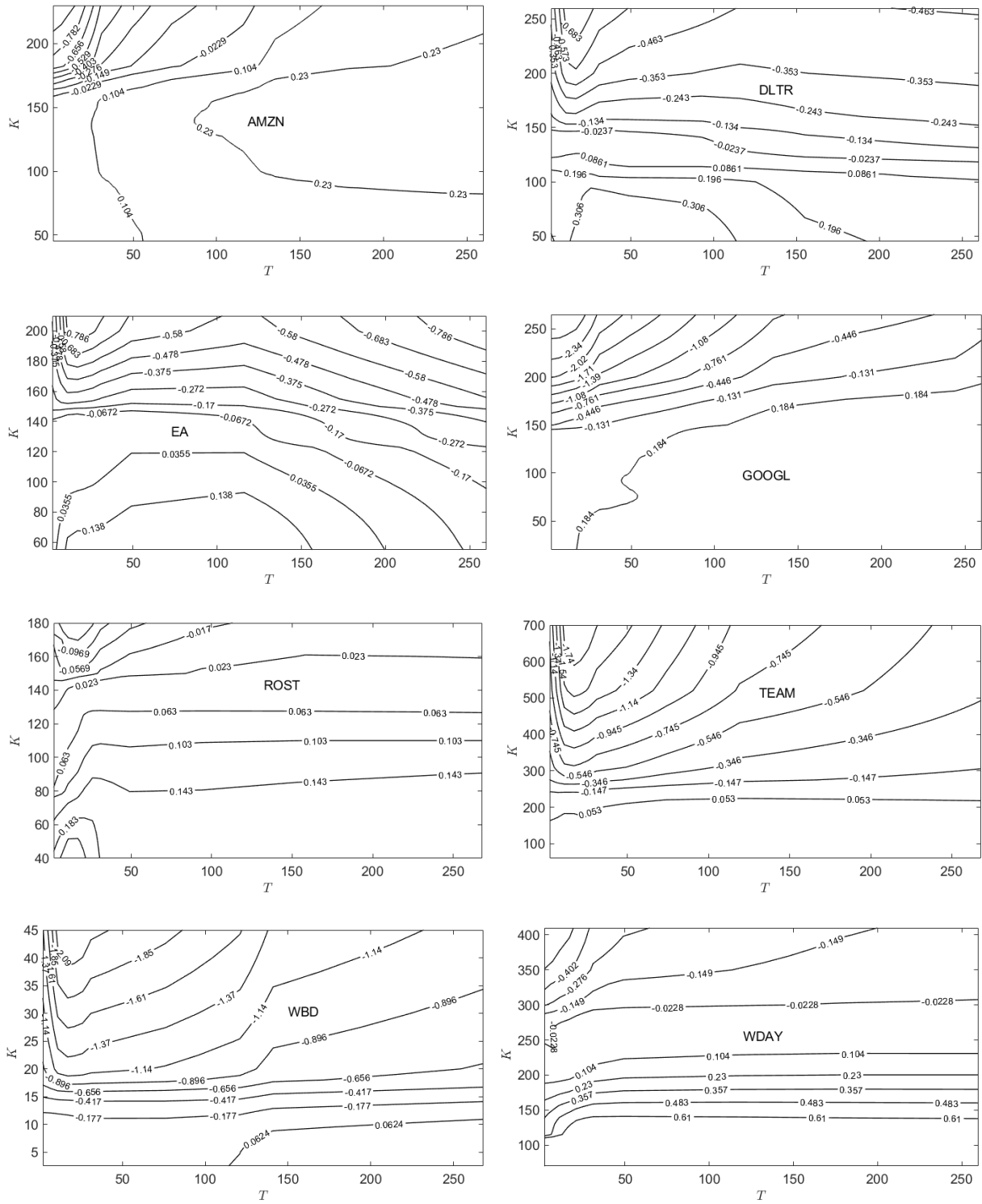
Figure C4. Contours of $\gamma^{(\text{ESG,imp})}$ for the indicated stocks with $Z_t^{(X,\wedge\text{NDX})} < 0$ on t = 01/02/2024.
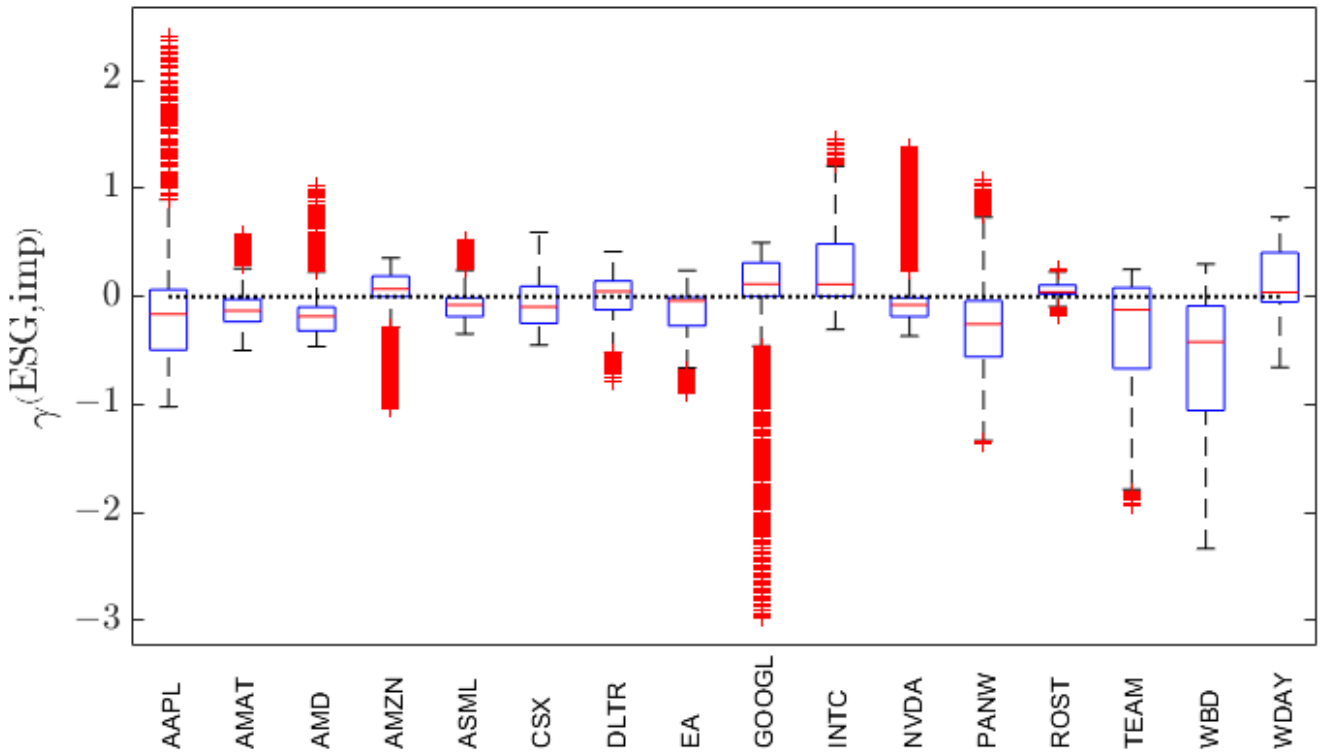
Figure C5. Box-whisker summaries of the distribution of $\gamma^{(ESG,imp)}$ values for all 16 stocks studied. The horizontal dotted-line indicates the value $\gamma^{(ESG,imp)} = 0$.

Figure C5 presents the box-whisker summaries of the distributions of $\gamma^{(ESG,imp)}$ values for each of the 16 stocks.

Appendix D. Plots of $a_t^{(\text{imp})}$
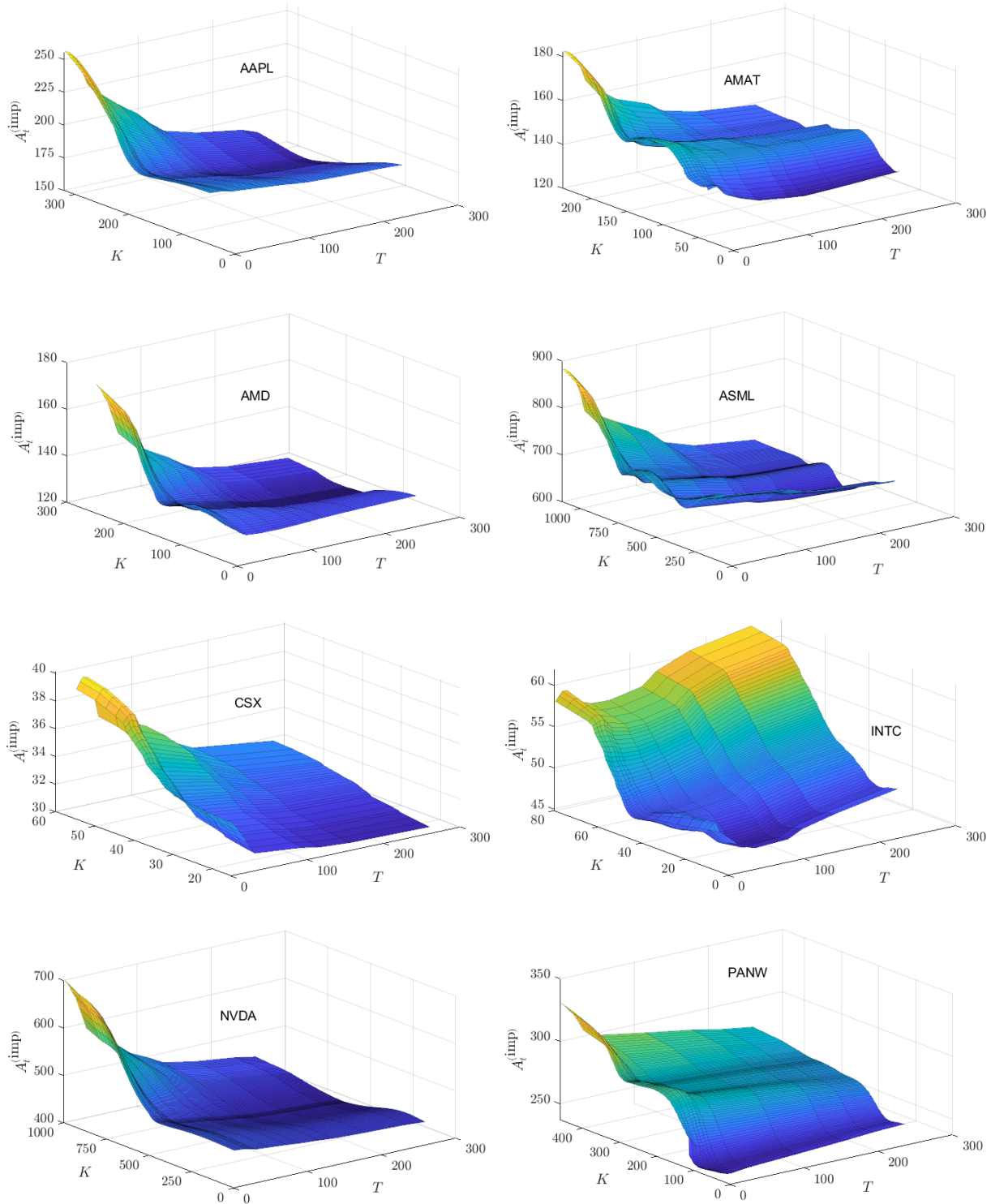
Figure D1. Surfaces of $A_t^{(\text{imp})}$ for the indicated stocks with $Z_t^{(X;^\wedge\text{NDX})} > 0$ on t = 01/02/2024.

Figure D1 plots $A_t^{(\text{imp})}$ as a function of strike price K and time to maturity T for the eight companies for which $Z_t^{(X,^\wedge\text{NDX})} > 0$ for t = 01/02/2024, while Figure D2 plots the same for the eight companies for which $Z_t^{(X,^\wedge\text{NDX})} < 0$ for t = 01/02/2024.
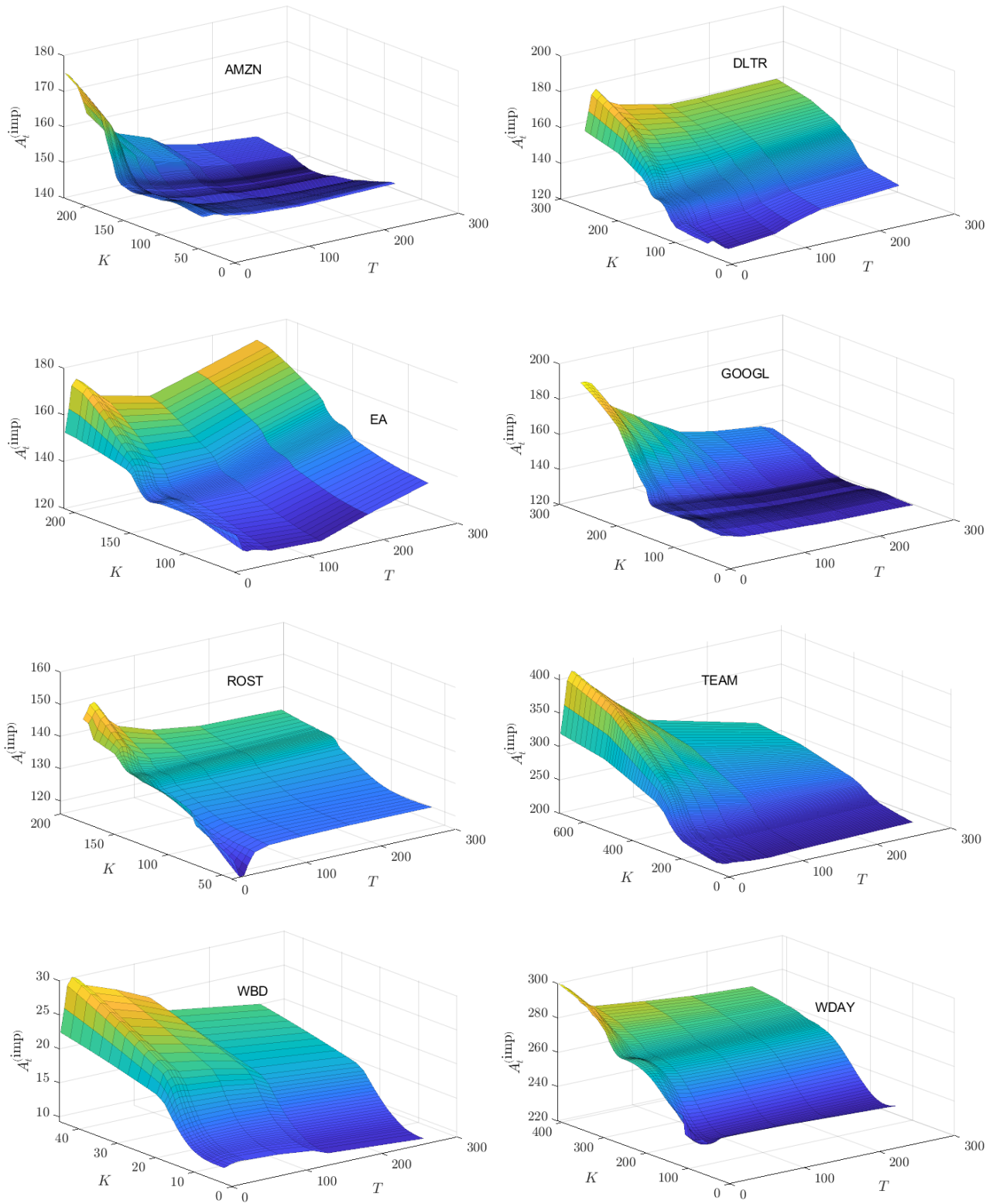
Figure D2. Surfaces of $A_t^{(\mathrm{imp})}$ for the indicated stocks with $Z_t^{(X,\wedge \mathrm{NDX})} < 0$ on t = 01/02/2024.
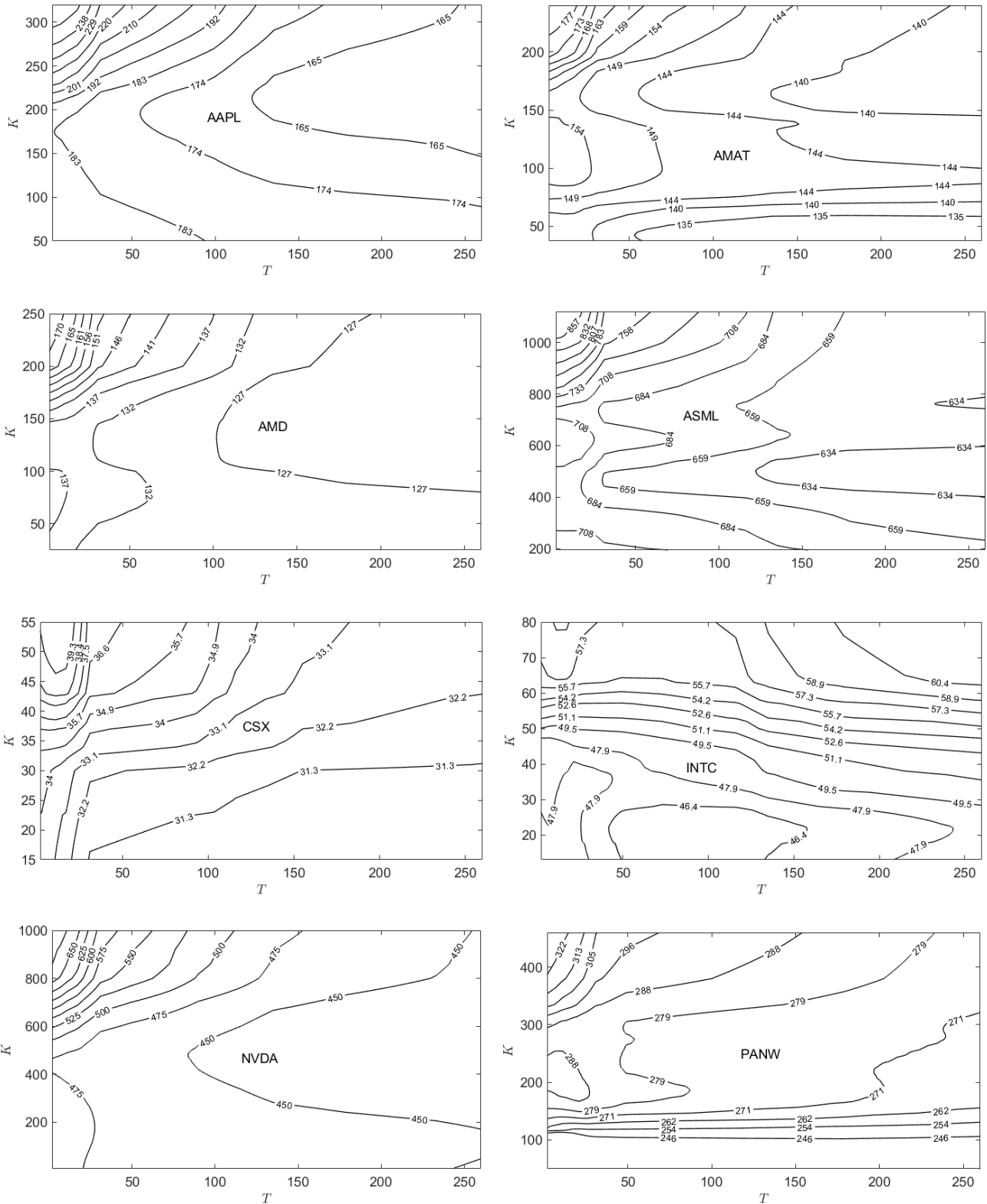
Figure D3. Contours of $A_t^{\text{(imp)}}$ for the indicated stocks with $Z_t^{(X;\wedge\text{NDX})} > 0$ on t = 01/02/2024.

Figure D3 plots contours of $A_t^{\text{(imp)}}$ as a function of strike price K and time to maturity T for the eight companies for which $Z_t^{(X,\wedge\text{NDX})} > 0$ for t = 01/02/2024 while Figure D4 plots the same for the eight companies for which $Z_t^{(X,\wedge\text{NDX})} < 0$ for t = 01/02/2024.
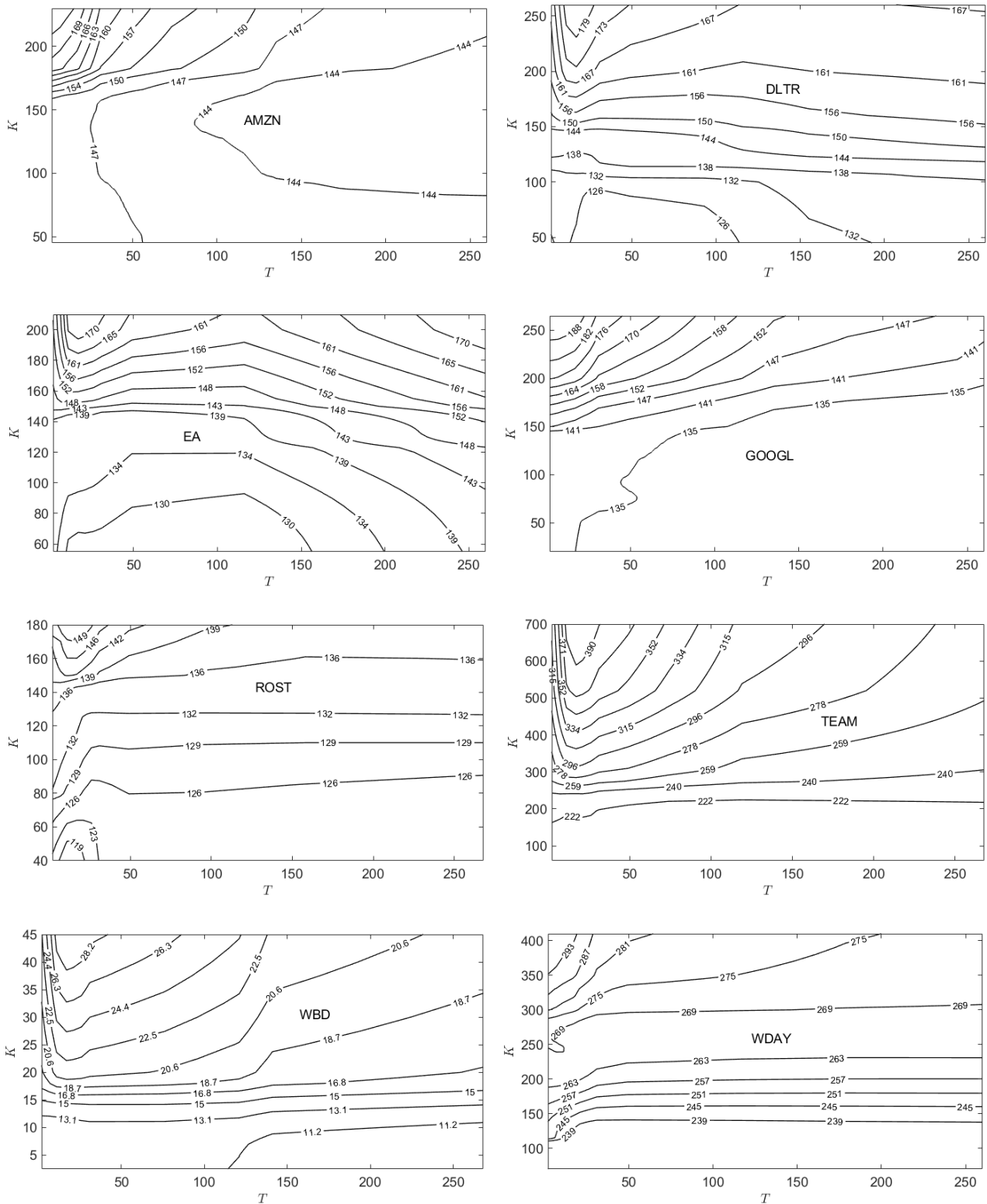
Figure D4. Contours of $A_t^{(\mathrm{imp})}$ for the indicated stocks with $Z_t^{(X,\wedge\mathrm{NDX})} < 0$ on t = 01/02/2024.

REFERENCES

1. Bachelier L. Théorie de la spéculation [Theory of speculation]. Ann Sci Ecole Norm S. 1900;3(17):21-86. French.

2. Black F, Scholes M. The pricing of options and corporate liabilities. J Political Econ. 1973;81(3):637-54.

3. Merton R. Theory of rational option pricing. Bell J Econ Manage Sci. 1973;4:141-83.

4. Rachev ST, Asare Nyarko N, Omotade B, Yegon P. Bachelier's market model for ESG asset pricing. J Risk Financ Manag. 2024;17(12):553.

5. Lindquist WB, Rachev ST, Gnawali J, Fabozzi FJ. Dynamic asset pricing in a unified Bachelier–Black–Scholes–Merton model. Risks. 2024;12:375.

6. Del Mar Miralles-Quiros M, Miralles-Quiros JL, Guia Arraiano I. Sustainable development, sustainability leadership and firm valuation: Differences across Europe. Bus Strateg Environ. 2017;26(7):1014-28.

7. Fulton M, Kahn B, Sharples C. Sustainable investing: Establishing long-term value and performance. Available from: http://dx.doi.org/10.2139/ssrn.2222740. Accessed on 10 Apr 2025.

8. Hu Y, Shirvani A, Stoyanov SV, Kim YS, Fabozzi FJ, Rachev ST. Option pricing in markets with informed traders. Int J Theor Appl Fin. 2020;23(06):2050037.

9. Asare Nyarko N, Divelgama B, Gnawali J, Omotade B, Rachev ST, Yegon P. Exploring Dynamic Asset Pricing within Bachelier's Market Model. J Risk Financ Manag. 2023;16(8):352.

10. Osborne M. Brownian motion in the stock market. Oper Res. 1959;7:145-73.

11. Alexander SS. Price movements in speculative markets: Trends or random walks. Ind Manag Rev. 1961;2:7-26.

12. Alexander SS. Price movements in speculative markets: Trends of random walks, Number 2. Ind Manag Rev. 1964;5:25-46.

13. Cootner P. The Random Character of Stock Market Prices. Cambridge (US): MIT Press; 1964.

14. Fama E. The behavior of stock market prices. J Bus. 1965;38:34-105.

15. Fama E. Efficient capital markets: A review of theory and empirical work. J Financ. 1970;25:383-417.

16. Fama E. Efficient Capital Markets: II. J Financ. 1991;46:1575-617.

17. Fama E. Random walks in stock market prices. Financ Anal J. 1995;51:75-80.

18. Jensen M. Some anomalous evidence regarding market efficiency. J Financ Econ. 1978;6(2/3):95-101.

19. Abu-Mostafa Y, Atiya A. Introduction to financial forecasting. Appl Intell. 1996;6:205-13.

20. Leung M, Daouk H, Chen AS. Forecasting stock indices: A comparison of classification and level estimation models. Int J Forecasting. 2000;16:173-90.

21. Malkiel B. The Efficient Market Hypothesis and its critics. J Econ Perspect. 2003;17:59-82.

22. Shiller RJ. From efficient markets theory to behavioral finance. J Econ Perspect. 2003;17:83-104.

23. Chung J, Hong Y. Are the directions of stock price changes predictable? A generalized cross-spectral approach. Available from: https://ideas.repec.org/p/ecm/nawm04/469.html. Accessed on 10 Apr 2025.

24. Campbell J, Thomson S. Predicting the equity premium out of sample: Can anything beat the historical average? Rev Financ Stud. 2008;21:1509-31.

25. Ang A, Goetzmann W, Schaefer S. The Efficient Market Theory and evidence:

Implications for active investment management. Found Trends Finance. 2010;5(3):157-242.

26. Cervelló-Royo R, Guijarro F, Michniuk K. Stock market trading rule based on pattern recognition and technical analysis: Forecasting the DJIA index with intraday data. Expert Syst Appl. 2015;42:5963-75.

27. Naseer M, Yasir T. The efficient market hypothesis: A critical review of the literature. IUP J Financ Risk Manag. 2014;12:48-63.

28. Qiu M, Song Y. Predicting the direction of stock market index movement using an optimized artificial neural network model. PLoS One. 2016;11(5):e0155133.

29. Chong E, Chulwoo H, Frank C. Deep learning networks for stock market analysis and prediction: Methodology, data representations, and case studies. Expert Syst Appl. 2017;83:187-205.

30. Rubén A, García J, Guijarro F, Peris A. A dynamic trading rule based on filtered flag pattern recognition for stock market price forecasting. Expert Syst Appl. 2017;81:177-92.

31. Zhong X, Enke D. Forecasting daily stock market return using dimensionality reduction. Expert Syst Appl. 2017;67:126-39.

32. Zhong X, Enke D. Predicting the daily return direction of the stock market using hybrid machine learning algorithms. Financ Innov. 2019;5(1):1-20.

33. Shah D, Isah H, Zulkernine F. Stock market analysis: A review and taxonomy of prediction techniques. Int J Financ Stud. 2019;7:26.

34. Chakravarty S, Gulen H, Mayhew S. Informed trading in stock and option markets. J Financ. 2004;59(3):1235-57.

35. Collin-Dufresne P, Fos V, Muravyev D. Informed trading in the stock market and option-price discovery. J Financ Quant Anal. 2021;56(6):1945-84.

36. Turkington J, Walsh D. Informed traders and their market preference: Empirical evidence from prices and volumes of options and stock. Pacific-Basin Financ J. 2000;8(5):559-85.

37. Billingsley P. Probability and Measure. 3rd ed. New York (US): Wiley; 1995.

38. Duffie D. Dynamic Asset Pricing Theory. 3rd ed. Princeton (US): Princeton University Press; 2001.

39. Yahoo Finance. https://finance.yahoo.com/. Accessed on 10 Apr 2025.

40. Slickcharts. https://www.slickcharts.com/nasdaq100. Accessed on 10 Apr 2025.

41. US Treasury. https://home.treasury.gov/resource-center/data-chart-center/interest-rates/TextView?type=daily_treasury_yield_curve&field_tdr_date_value=2024. Accessed on 10 Apr 2025.

42. Robinson D. Entropy and uncertainty. Entropy. 2008;10:493-506.

43. Rioul O. This is IT: A primer on Shannon's entropy and information. In: Duplantier B, Rivasseau V, editors. Information Theory. Cham (Switzerland): Birkhäuser; 2018. p. 49-86.